

Craig Roberts



Physics Division

Bound-state Problem in Continuum QCD



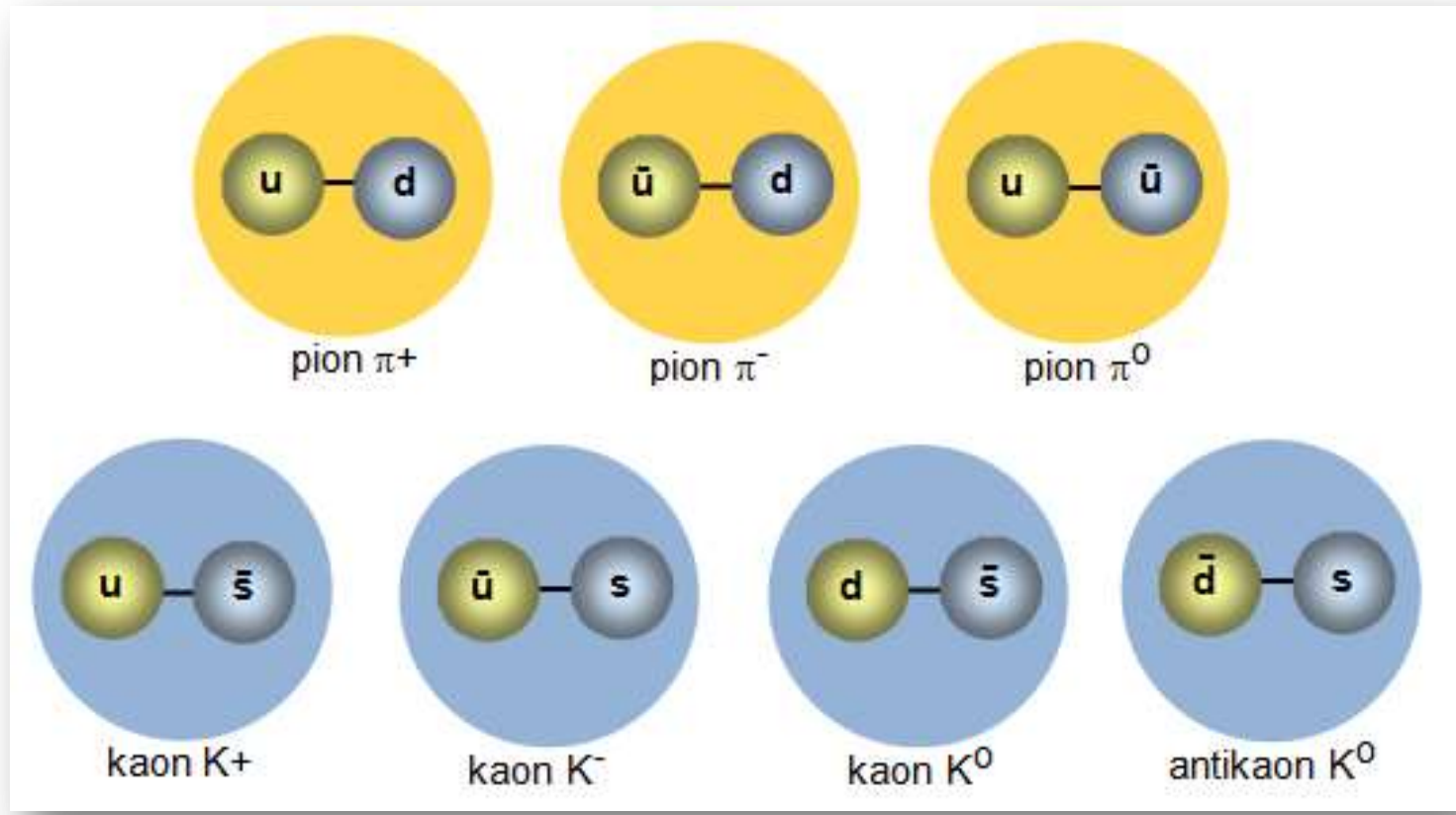
Overarching Science Challenges for the coming decade: 2014-2023

- Discover the meaning of confinement
- Determine its connection with DCSB
(dynamical chiral symmetry breaking)
- Expose and explain their signals in observables
... so experiment and theory together can map the nonperturbative behaviour of the strong interaction

In my view, it is unlikely that two phenomena, so critical in the Standard Model and tied to the dynamical generation of a single mass-scale, can have different origins and fates.

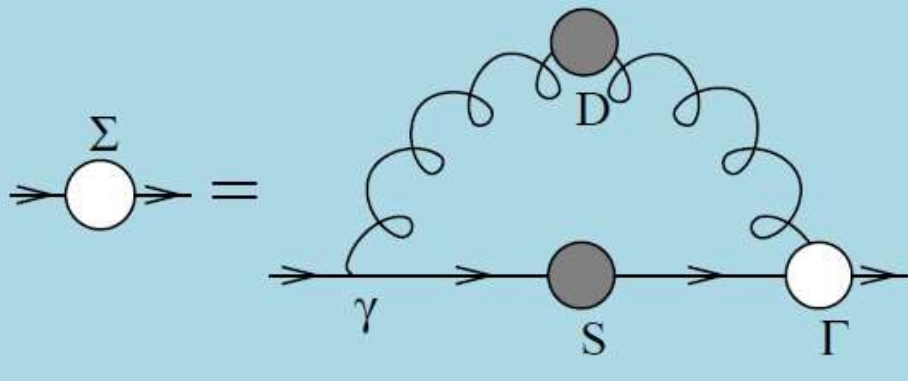
Immediate Science Challenges for the coming decade: 2014-2023

- Exploit opportunities provided by new data on hadron elastic and transition form factors
 - *Chart infrared evolution of QCD's coupling and dressed-masses*
 - *Reveal correlations that are key to baryon structure*
 - *Expose facts & fallacies in modern descriptions of hadron structure*
- Precision experimental study of (far) valence region, and theoretical computation of distribution functions and distribution amplitudes
 - *Computation is critical*
 - *Without it, no amount of data will reveal anything about the theory underlying the phenomena of strong interaction physics*



Mesons

Dressed-quark propagator



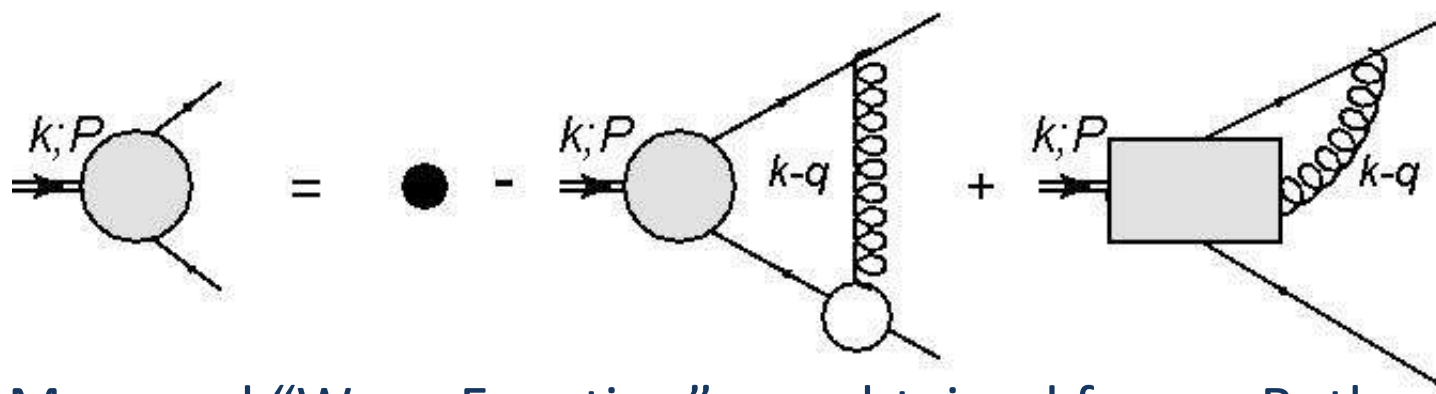
- Starting point for the continuum bound-state problem.
- Two crucial elements, derived from the contraction

$$D_{\mu\nu}(k-q) \Gamma_\nu(q, k)$$

- ✓ Dressed gluon propagator
- ✓ Dressed quark-gluon vertex
- Qin-Chang interaction is a representation of the gluon propagator that is consistent with all available information on QCD's gauge sector.
 - Maris-Tandy interaction fails that test in the far infrared.
- Dressed-quark-gluon vertex
 - That is where the *action* is!

Interaction model for the gap equation
Si-xue Qin, Lei Chang *et al.* [arXiv:1108.0603 \[nucl-th\]](https://arxiv.org/abs/1108.0603), *Phys. Rev. C* **84** (2011) 042202(R) [5 pages]

Mesons in Quantum Field Theory



- Mass and “Wave Function” are obtained from a Bethe-Salpeter equation
 - Generalisation of the Lippmann-Schwinger equation
- General structure is complicated, any truncation must preserve the crucial symmetries: Poincaré-covariance, vector and axial-vector Ward-Green-Takahashi identities
- The pion ... Nature’s strong-interaction messenger ... is a critical example

Sketching the Bethe-Salpeter kernel, Lei Chang and Craig D. Roberts,
[arXiv:0903.5461 \[nucl-th\]](https://arxiv.org/abs/0903.5461), [Phys. Rev. Lett. 103 \(2009\) 081601](https://doi.org/10.1103/PhysRevLett.103.081601) (4 pages)

Ward-Green-Takahashi Identities

Craig Roberts: Bound state problem in continuum QCD (87p)

LETTERS TO THE EDITOR

ties and the latter in studying atmospheric ionization at ground level. These increases in ionization are considered to be due to radioactive matter brought down with the rain. Between 0935 and 1900 hr, GMT on November 20 at Ottawa precipitation was falling. The precipitation started as snow and changed to rain about 1400 hr. Compared with the results of Dean and Watt and McNish the 35 percent increase in the soft component registered at Ottawa by counters seems too high to be explained in the same way, unless there was an exceptionally high density of radioactive matter in the atmosphere at the time. An alternative, but not very likely explanation, might be that there was a burst of hard gamma-rays or some other radiation which would increase the number of soft shower particles without any appreciable effect on the hard component.

An interesting feature of the November 19 increase is the difference between the measurements at the various stations, particularly between Resolute and Godhavn (geomagnetic latitude 80°). These two stations are about 900 miles apart and the differences confirm previous indications that sudden increments in cosmic-ray intensity occur over a limited area. The lack of a sudden decrease after the increment is unusual, since a decrease has been reported on previous occasions.

The cooperation of the Department of Transport of the Government of Canada is appreciated for supplying facilities at Resolute and for weather information.

- J. A. Thivierge, *Canadian Weather Review* **29**, 1095 (1949).
 *Forbush, Stachowitz and Schon, *Bull. Am. Phys. Soc.* **25**, No. 1, 13 (1939).
 *J. L. Chakraborty and R. D. Chamberlin, *Ind. J. Phys.* **23**, 523 (1949).
 *Forbush, Gill and Villars, *Rev. Mod. Phys.* **21**, 64 (1949).
 *R. L. Dean, *Phys. Rev.* **49**, 197 (1936).
 *G. H. Watt and A. G. McNish, *Monthly Weather Rev.* **62**, 1 (1934).

Now substitute this identity into Eqs. (91) and (93) of reference 1. One finds

$$\Lambda_a = Z_1^{-1} [(1 - Z_1) \gamma_a + \lambda_a c], \quad \Sigma^* = Z_2^{-1} [(Z_2 - 1) S_F^{-1} + S_F^{-1} S_C / 2 \pi].$$

We have

$$-(1/2\pi) Z_2^{-1} [(Z_2 - 1) 2\pi \gamma_a + \gamma_a S_C + (\gamma_a \beta_a - iK_0)(\partial S_C / \partial \beta_a)] \\ - Z_2^{-1} [(1 - Z_2) \gamma_a + \lambda_a c(\beta_a, \gamma_a)].$$

Now put

$$\gamma_a \beta_a = (E_{\lambda_a})^2 - K_0^2.$$

The convergent parts of these equations then vanish and there is left the relation

$$-(1/2\pi) Z_2^{-1} (Z_2 - 1) 2\pi \gamma_a = Z_2^{-1} (1 - Z_2) \gamma_a,$$

which reduces immediately to $Z_1 = Z_2$.

* F. J. Dyson, *Phys. Rev.* **15**, 1736 (1949).

The Partial Molal Entropy of Superfluid in Pure He⁴ below the λ-Point

O. K. Rice

*Department of Chemistry, University of North Carolina,
Chapel Hill, North Carolina*

March 3, 1959

In a recent article¹ (the notation of which is retained here, except that subscripts 4 and 4s refer to normal fluid and superfluid, respectively, in place of 1 and 2), I have considered the thermodynamics of liquid helium on the two-fluid theory, taking account of the fact that if two "phases" or "components," the normal fluid and the superfluid, exist together they must be in equilibrium with each other. On this basis, using the assumed relation² which states that the total molal entropy S at any temperature is the mole fraction x_{4s} of normal fluid times the molal entropy S_{4s} at the λ-point

$$S = x_{4s} S_{4s} + (1 - x_{4s}) S_{4n}, \quad (1)$$

using the empirical relation for S as a function of temperature

$$S = S_{4s}(T/T_b)^{\alpha} \quad (2)$$

(with $\alpha \sim 5.6$), and assuming that the partial molal enthalpy of superfluid, \bar{H}_{4s} , is independent of temperature (at essentially constant pressure), and independent of x_{4s} (i.e., there is no heat of mixing), I derived the equation for the partial molal entropy of superfluid

$$S_{4s} = S_{4s} x_{4s} / (r + 1), \quad (3)$$

However, as I remarked in reference 1, there are some approximations involved in this procedure. Equation (1) is based on the assumption that below T_b the entropy is contributed solely by the normal fluid, whose molal entropy is always set equal to the constant S_{4n} , thus neglecting any temperature dependence. Furthermore, there is an implied inconsistency, since Eq. (1) assumes no entropy of mixing while Eq. (3) implies that there is a mixing entropy. In fact, in the following letter we shall show that we may derive a somewhat different expression for S from Eq. (3). We shall, therefore, discard Eq. (1) and turn to a consideration of the enthalpies.

If \bar{H}_{4s} is independent of x_{4s} , then \bar{H}_{4s} must be also, and we have $\bar{H}_{4s} = \bar{H}_{4n}$, where \bar{H}_{4n} is the enthalpy of pure normal helium. We can write for the total molal enthalpy³

$$\bar{H} = x_{4s} \bar{H}_{4s}. \quad (4)$$

We will now proceed to derive an expression for \bar{H}_{4s} in a somewhat more direct way than in reference 1, using Eq. (4) in place of Eq. (1). Since $\bar{F} = \bar{H} - TS$ and $\mu_{4s} = \bar{H}_{4s} - T\bar{S}_{4s} = -TS$, the condition for internal equilibrium, $F = \mu_{4s}$, gives

$$\bar{S}_{4s} = \bar{S} - \bar{H}/T.$$

Longitudinal Axial-Vector Ward-Green-Takahashi Identity

$$\begin{aligned}
 P_\mu \Gamma_{5\mu}^l(k; P) &= \mathcal{S}^{-1}(k_+) \frac{1}{2} \lambda_f^l i \gamma_5 + \frac{1}{2} \lambda_f^l i \gamma_5 \mathcal{S}^{-1}(k_-) \\
 &\quad - M_\zeta i \Gamma_5^l(k; P) - i \Gamma_5^l(k; P) M_\zeta
 \end{aligned}$$

Axial-Vector vertex
 Satisfies an inhomogeneous
 Bethe-Salpeter equation

Quark propagator
 satisfies a
 gap equation

*Kernels of these equations are completely different
 But they must be intimately related*

- This class of identities have been known for more than 60 years
- They have been used for 19 years in order to construct a symmetry-preserving kernel for the Bethe-Salpeter equation
- For the last 5 years we've known how to construct a symmetry preserving kernel given an arbitrary quark-gluon vertex



What is Γ_μ ?

Craig Roberts: Bound state problem in continuum QCD (87p)

Sao Paulo: II Workshop on Perspectives in
Nonperturbative QCD, 12-13 May 14

Takahashi. (1985), Canonical quantization and generalized Ward relations: Foundation of nonperturbative approach, Print-85-0421 (Alberta).

[Transverse Ward-Takahashi identity, anomaly and Schwinger-Dyson equation](#) - Kondo, Kei-Ichi Int.J.Mod.Phys. A12 (1997) 5651-5686 hep-th/9608100 CHIBA-EP-94, OUTP-96-30-P

[Transverse Ward-Takahashi identity for the fermion boson vertex in gauge theories](#) - He, Han-Xin et al. Phys.Lett. B480 (2000) 222-228

[Transverse vector vertex function and transverse Ward-Takahashi relations in QED](#) - He, Han-Xin Commun.Theor.Phys. 46 (2006) 109-112

[Transverse Ward-Takahashi relation for the fermion-boson vertex function in four-dimensional Abelian gauge theory](#) - He, Han-Xin Int.J.Mod.Phys. A22 (2007) 2119-2132

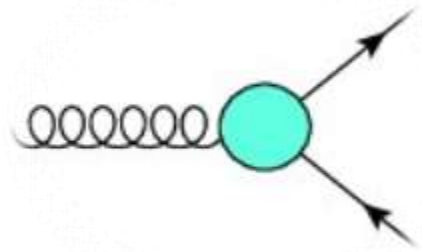
[Nonperturbative fermion boson vertex function in gauge theories](#) - He, Han-xin hep-th/0202013

[Checking the transverse Ward-Takahashi relation at one loop order in 4-dimensions](#) - Pennington, M.R. et al. J.Phys. G32 (2006) 2219-2234 hep-ph/0511254 DCPT-05-130, IPPP-05-65

[Transverse Ward-Takahashi relation for the fermion-boson vertex to one-loop order](#) - He, Han-Xin et al. J.Mod.Phys. A21 (2006) 2541-2551

Transverse Ward-Green-Takahashi Identities

Ward-Green-Takahashi identities



- Gauge principle is fundamental in formulating the Standard Model.
- Fermion-gauge-boson couplings are the inescapable consequence and the primary determining factor for observable phenomena.
- Vertices describing such couplings are simple in perturbation theory; yet existence of strong-interaction bound-states guarantees that many phenomena within the SM are nonperturbative.
- Unified treatment and solution of the familiar longitudinal Ward-Green-Takahashi identity and its less well known transverse counterparts.
- **Novel consequences for the dressed-fermion-gauge-boson vertex**

Practical corollaries of transverse Ward-Green-Takahashi identities, Si-xue Qin et al. [arXiv:1302.3276](https://arxiv.org/abs/1302.3276) [nucl-th], Phys. Lett. B 722 (2013) pp. 384–388



Practical corollaries of transverse Ward–Green–Takahashi identities

Si-xue Qin^{a, b}, Lei Chang^c, Yu-xin Liu^a, , Craig D. Roberts^{d, e}, , Sebastian M. Schmidt^f

- Longitudinal WGT identity expresses properties of the divergence of the vertex
 - Transverse identities relate to its *curl* (as Faraday's law of induction involves an electric field)
 - The last two terms in each identity arise in computing the momentum space expression of a nonlocal axial-vector/vector vertex, whose definition involves a gauge-field-dependent line integral
 - But ... practical progress can be made without knowing their precise forms
- $$q_\mu \Gamma_v(k, p) - q_v \Gamma_\mu(k, p) = S^{-1}(p) \sigma_{\mu\nu} + \sigma_{\mu\nu} S^{-1}(k) + 2im \Gamma_{\mu\nu}(k, p) + t_\lambda \varepsilon_{\lambda\mu\nu\rho} \Gamma_\rho^A(k, p) + A_{\mu\nu}^V(k, p),$$
- $$q_\mu \Gamma_v^A(k, p) - q_v \Gamma_\mu^A(k, p) = S^{-1}(p) \sigma_{\mu\nu}^5 - \sigma_{\mu\nu}^5 S^{-1}(k) + t_\lambda \varepsilon_{\lambda\mu\nu\rho} \Gamma_\rho(k, p) + V_{\mu\nu}^A(k, p),$$



Practical corollaries of transverse Ward–Green–Takahashi identities

Si-xue Qin^{a, b}, Lei Chang^c, Yu-xin Liu^a, , Craig D. Roberts^{d, e}, , Sebastian M. Schmidt^f

- Using symmetries alone, it is readily established that DCSB demands that dressed fermions possess anomalous chromo- and electro-magnetic moments, which are large on the domain within which DCSB is effective
- This is the “final” word.
- Evidence had slowly been accumulating since 1985

[Anomalous Magnetic Moment Of Light Quarks And Dynamical Symmetry Breaking](#) - Singh, J.P. Phys.Rev. D31 (1985) 1097-1108

[Anomalous quark chromomagnetic moment induced by instantons](#) - Kocherov, N.I. Phys.Lett. B426 (1998) 149-153 hep-ph/9610551 KOBE-FHD-96-01, C96-09-02.3

[The Anomalous magnetic moment of quarks](#) - Bicudo, Pedro J.A. et al. Phys.Rev. C59 (1999) 1107-1112 hep-ph/9806243

[Dressed-quark anomalous magnetic moments](#) - Chang, Lei et al. Phys.Rev.Lett. 106 (2011) 072001 arXiv:1009.3458 [nucl-th]

[Dynamical chiral symmetry breaking and the fermion–gauge-boson vertex](#) - Bashir, A. et al. Phys.Rev. C85 (2012) 045205 arXiv:1112.4847 [nucl-th]

Dynamically generated AMM

- Simple vertex in perturbation theory γ_μ
 \rightarrow 12 distinct terms when strong interactions are turned on
- Amongst them, one with the unique structure; i.e., an anomalous magnetic moment term

$$\propto \sigma_{\mu\nu} k_\nu \frac{dB(k^2)}{dk^2}$$

- Follows, algebraically, that gauge theories coupled to fermions with a dynamically generated mass MUST possess an anomalous (chromo/electro)-magnetic moment, whose magnitude is driven by the strength of DCSB

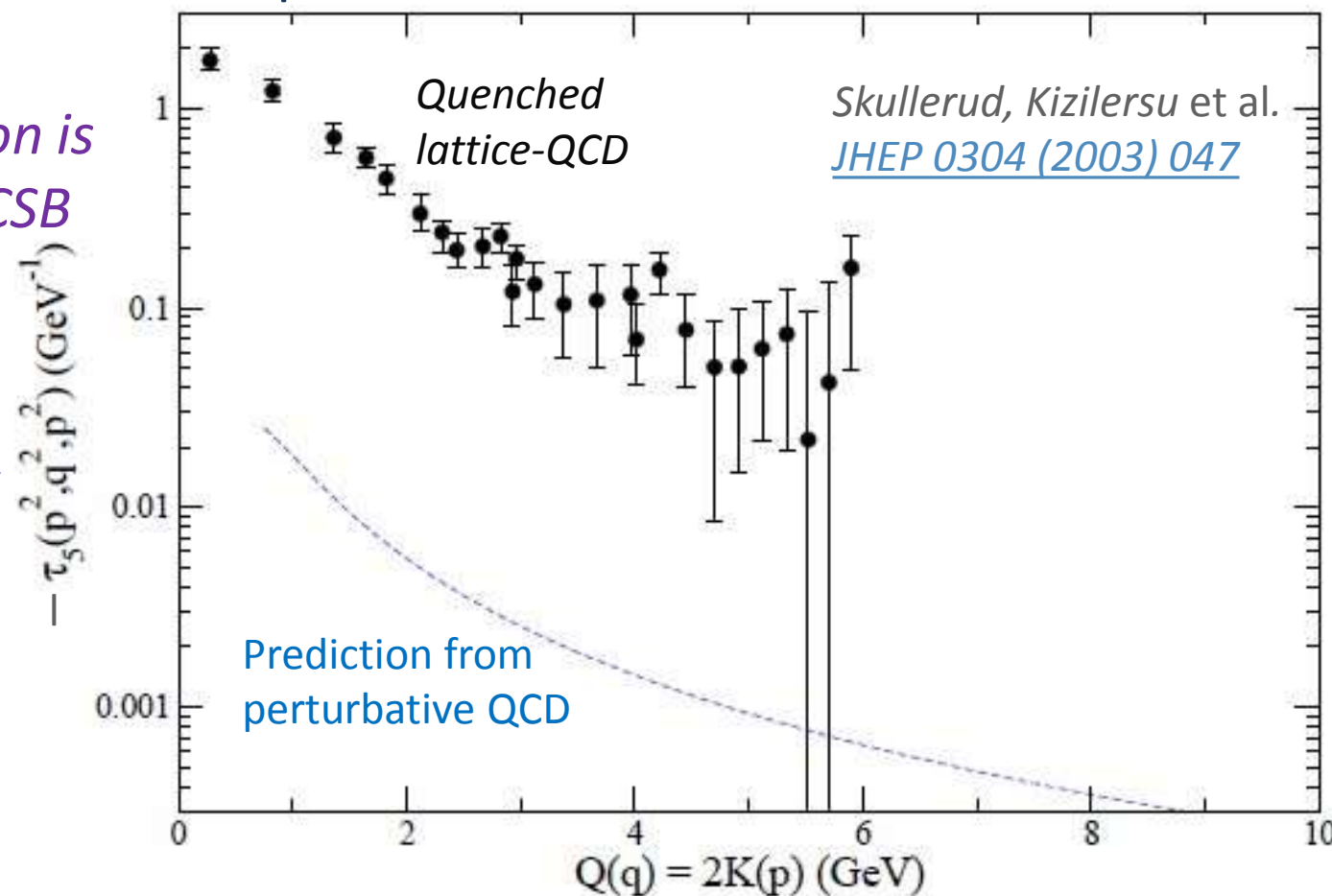
- Lattice-QCD
 - $m = 115 \text{ MeV}$
- Nonperturbative result is *two orders-of-magnitude* larger than the perturbative computation
 - *This level of magnification is typical of DCSB*
 - *cf.*

Quark mass function:

$$M(p^2=0) = 400 \text{ MeV}$$

$$M(p^2=10 \text{ GeV}^2) = 4 \text{ MeV}$$

Dressed-quark anomalous chromomagnetic moment



Modern $\Gamma_\mu(q,k)$

Tracing masses of ground-state light-quark mesons

Phys. Rev. C **85**, 052201(R) – Published 7 May 2012

Lei Chang and Craig D. Roberts

- Describes the best-informed vertex available today

- Contains all the Ball-Chiu terms

They are unique as the kinematic-singularity-free solution of the longitudinal vector WGT identity

- And two of the terms critical for expressing the AMMs

$$\Gamma_\mu^{\text{acm}}(p_1, p_2) = \Gamma_\mu^{\text{acm}4}(p_1, p_2) + \Gamma_\mu^{\text{acm}5}(p_1, p_2), \quad (8)$$

$$\text{with } (k = p_1 - p_2, T_{\mu\nu} = \delta_{\mu\nu} - k_\mu k_\nu / k^2, a_\mu^\text{T} := T_{\mu\nu} a_\nu)$$

$$\Gamma_\mu^{\text{acm}4} = [\ell_\mu^\text{T} \gamma \cdot k + i \gamma_\mu^\text{T} \sigma_{\nu\rho} \ell_\nu k_\rho] \tau_4(p_1, p_2), \quad (9)$$

$$\Gamma_\mu^{\text{acm}5} = \sigma_{\mu\nu} k_\nu \tau_5(p_1, p_2), \quad (10)$$

$$\tau_4 = \frac{2\tau_5(p_1, p_2)}{\mathcal{M}(p_1^2, p_2^2)}, \quad (11)$$

- The chromo AMM is crucial to explaining the splitting between parity partners, such as a_1 - ρ mass splitting, and connecting it with DCSB



Impact of Symmetry

Craig Roberts: Bound state problem in continuum QCD (87p)

Sao Paulo: II Workshop on Perspectives in Nonperturbative QCD, 17
12-13 May 14

Pion's Goldberger -Treiman relation

- Pion's Bethe-Salpeter amplitude

Solution of the Bethe-Salpeter equation

$$\Gamma_{\pi^j}(k; P) = \tau^{\pi^j} \gamma_5 \left[iE_\pi(k; P) + \gamma \cdot P F_\pi(k; P) \right. \\ \left. + \gamma \cdot k k \cdot P G_\pi(k; P) + \sigma_{\mu\nu} k_\mu P_\nu H_\pi(k; P) \right]$$

*Pseudovector components necessarily nonzero.
Cannot be ignored!*

- Dressed-quark propagator

$$S(p) = \frac{1}{i\gamma \cdot p A(p^2) + B(p^2)}$$

- Axial-vector Ward-Takahashi identity entails

$$f_\pi E_\pi(k=0) = B(k^2)$$

Owing to DCSB
& Exact in
Chiral QCD

**Miracle: two body problem solved,
almost completely, once solution of
one body problem is known**

$$f_{H_5} m_{H_5}^2 = \rho_{H_5}^\zeta \mathcal{M}_{H_5}^\zeta$$

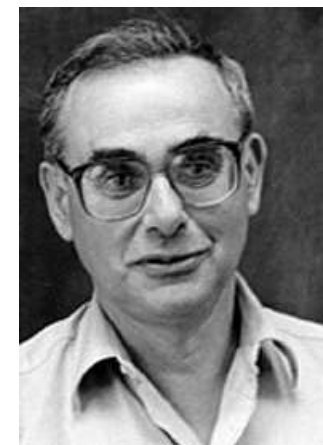
Enigma of mass

- The quark level Goldberger-Treiman relation shows that DCSB has a very deep and far reaching impact on physics within the strong interaction sector of the Standard Model; viz.,

Goldstone's theorem is fundamentally an expression of equivalence between the one-body problem and the two-body problem in the pseudoscalar channel.

$$f_\pi E_\pi(p^2) = B(p^2)$$

- This emphasises that Goldstone's theorem has a pointwise expression in QCD
- Hence, pion properties are an almost direct measure of the dressed-quark mass function.
- Thus, enigmatically, the properties of the *massless* pion are the cleanest expression of the mechanism that is responsible for almost all the visible mass in the universe.



Dichotomy of the pion Mass Formula for 0⁻ Mesons

$$f_{H_5} m_{H_5}^2 = \rho_{H_5}^\zeta \mathcal{M}_{H_5}^\zeta$$

- Mass-squared of the pseudoscalar hadron
- Sum of the current-quark masses of the constituents;
e.g., pion = $m_u^\zeta + m_d^\zeta$, where “ ζ ” is the renormalisation point

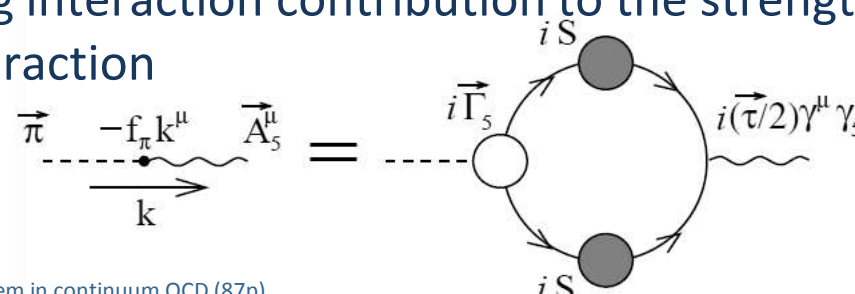
Dichotomy of the pion Mass Formula for 0^- Mesons

$$f_{H_5} m_{H_5}^2 = \rho_{H_5}^\zeta \mathcal{M}_{H_5}^\zeta$$

$f_{H_5} P_\mu = Z_2 \text{tr} \int \frac{d^4 q}{(2\pi)^4} \frac{1}{2} (T^{H_5})^t \gamma_5 \gamma_\mu S(q + \frac{1}{2}P) \Gamma_{H_5}(q; P) S(q - \frac{1}{2}P)$

- **Pseudovector projection of the Bethe-Salpeter wave function onto the origin in configuration space**

- Namely, the pseudoscalar meson's leptonic decay constant, which is the strong interaction contribution to the strength of the meson's weak interaction

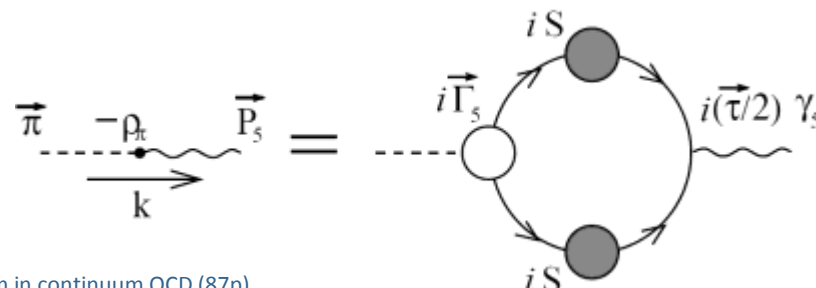


Dichotomy of the pion Mass Formula for 0^- Mesons

$$f_{H_5} m_{H_5}^2 = \rho_{H_5}^\zeta \mathcal{M}_{H_5}^\zeta$$

$$i\rho_{H_5} = Z_4 \text{tr} \int \frac{d^4 q}{(2\pi)^4} \frac{1}{2} (T^{H_5})^t \gamma_5 S(q + \frac{1}{2}P) \Gamma_{H_5}(q; P) S(q - \frac{1}{2}P)$$

- Pseudoscalar projection of the Bethe-Salpeter wave function onto the origin in configuration space
 - Namely, a pseudoscalar analogue of the meson's leptonic decay constant



Dichotomy of the pion Mass Formula for 0⁻ Mesons

$$f_{H_5} m_{H_5}^2 = \rho_{H_5}^\zeta \mathcal{M}_{H_5}^\zeta$$

➤ Consider the case of light quarks; namely, $m_q \approx 0$

- If chiral symmetry is dynamically broken, then

- $f_{H_5} \rightarrow f_{H_5}^0 \neq 0$
- $\rho_{H_5} \rightarrow -\langle \bar{q}q \rangle / f_{H_5}^0 \neq 0$

both of which are independent of m_q

➤ Hence, one arrives at the corollary *Gell-Mann, Oakes, Renner relation*

$$m_{H_5}^2 = 2m_q \frac{-\langle \bar{q}q \rangle}{f_{H_5}^0}$$

$$m_\pi^2 \propto m$$

The so-called “vacuum quark condensate.” It’s actually contained within hadrons.

1968

Radial excitations & Hybrids & Exotics

⇒ wave-functions with support at long-range

⇒ sensitive to confinement interaction

Understanding confinement “remains one of
The greatest intellectual challenges in physics”

Radial excitations of Pseudoscalar meson

- Hadron spectrum contains 3 pseudoscalars [$I^G(J^P)L = 1^-(0-)S$]
masses below 2GeV: $\pi(140)$; $\pi(1300)$; and $\pi(1800)$
the pion
- Constituent-Quark Model suggests that these states are
the 1st three members of an n^1S_0 trajectory;
i.e., ground state plus radial excitations
- But $\pi(1800)$ is narrow ($\Gamma = 207 \pm 13$); i.e., surprisingly long-lived
& decay pattern conflicts with usual quark-model expectations.
 - $S_{Q-bar Q} = 1 \oplus L_{Glue} = 1 \Rightarrow J = 0$
& $L_{Glue} = 1 \Rightarrow {}^3S_1 \oplus {}^3S_1$ (Q-bar Q) decays are suppressed
 - Perhaps therefore it's a hybrid?

exotic mesons: quantum numbers not possible for quantum mechanical quark-antiquark systems

hybrid mesons: normal quantum numbers but non-quark-model decay pattern

BOTH suspected of having “constituent gluon” content

Radial excitations of Pseudoscalar meson

$$f_{H_5} m_{H_5}^2 = \rho_{H_5}^\zeta \mathcal{M}_{H_5}^\zeta$$

Flip side: if no DCSB, then all pseudoscalar mesons decouple from the weak interaction!

- Valid for ALL Pseudoscalar mesons
 - When chiral symmetry is dynamically broken, then
 - ρ_{H_5} is finite and nonzero in the chiral limit, $M_{H_5} \rightarrow 0$
 - A “radial” excitation of the π -meson, is not the ground state, so
$$m_{\pi \text{ excited state}}^2 \neq 0 > m_{\pi \text{ ground state}}^2 = 0 \text{ (in chiral limit, } M_{H_5} \rightarrow 0\text{)}$$
- Putting this things together, it follows that

$$f_{H_5} = 0$$

for ALL pseudoscalar mesons, except $\pi(140)$,
in the chiral limit

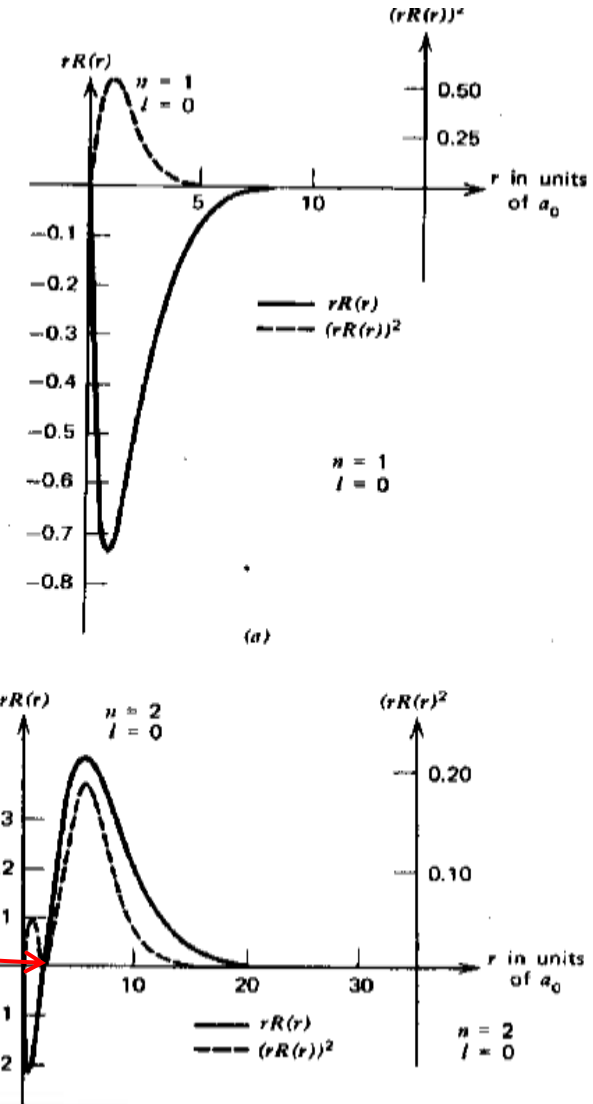
*Dynamical Chiral Symmetry Breaking – Goldstone’s Theorem – impacts upon **every** pseudoscalar meson*

Radial excitations of Pseudoscalar meson

- This is fascinating because in quantum mechanics, decay constants of a radial excitation are suppressed by factor of roughly $\frac{1}{3}$

- Radial wave functions possess a zero
- Hence, integral of “ $r R_{n=2}(r)^2$ ” is quantitatively reduced compared to that of “ $r R_{n=1}(r)^2$ ”

➤ **HOWEVER, ONLY A SYMMETRY CAN ENSURE THAT SOMETHING VANISHES COMPLETELY**



Lattice-QCD & radial excitations of pseudoscalar mesons

The suppression of $f_{\pi 1}$ is a useful benchmark that can be used to tune and validate lattice QCD techniques that try to determine the properties of excited state mesons.

- When we first heard about [this result] our first reaction was a combination of “that is remarkable” and “unbelievable”.

- CLEO: $\tau \rightarrow \pi(1300) + \nu_\tau$

$$\Rightarrow f_{\pi 1} < 8.4 \text{ MeV}$$

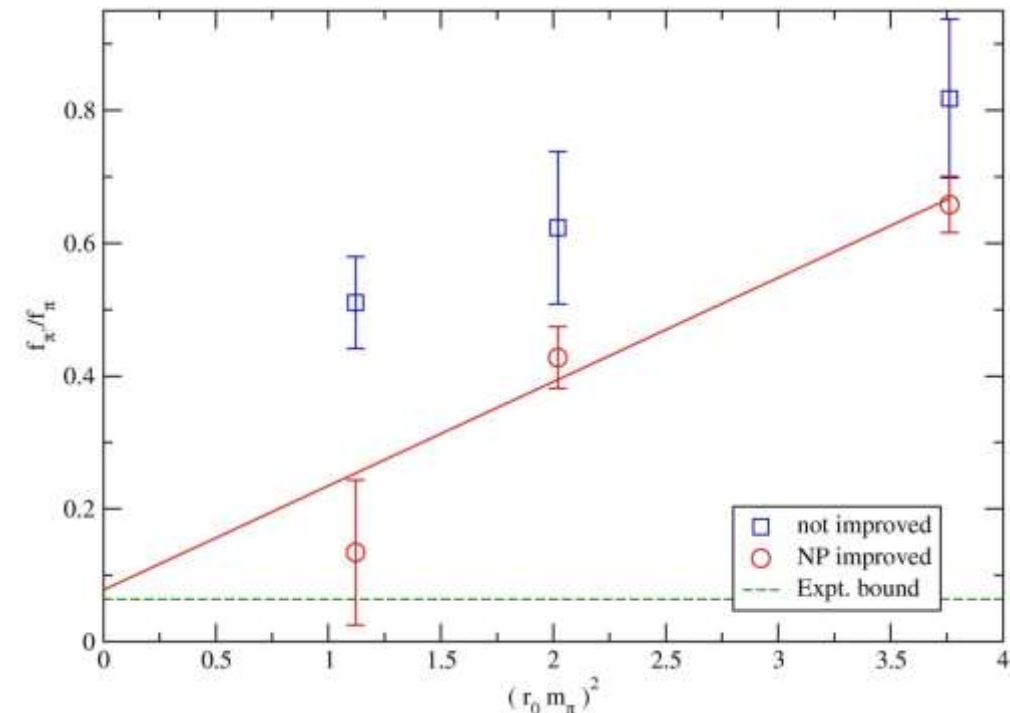
Diehl & Hiller

[hep-ph/0105194](https://arxiv.org/abs/hep-ph/0105194)

- Lattice-QCD check:
 $16^3 \times 32$ -lattice, $a \sim 0.1 \text{ fm}$,
two-flavour, unquenched

$$\Rightarrow f_{\pi 1}/f_\pi = 0.078 (93)$$

- Full ALPHA formulation is required to see suppression, because PCAC relation is at the heart of the conditions imposed for improvement (determining coefficients of irrelevant operators)



Some New Challenges

- Heavy-light systems using the DCSB-improved kernel
 - Rainbow-ladder kernel cannot work because cancellations required for its accuracy don't happen.
- Computation of spectrum of hybrid and exotic mesons
 - exotic mesons:** quantum numbers not possible for quantum mechanical quark-antiquark systems
 - hybrid mesons:** normal quantum numbers but non-quark-model decay pattern
 - BOTH** suspected of having “constituent gluon” content
 - It appears that this will need to be treated as a three-body problem (dressed-q+dressed-qbar+dressed-g) because best attempts so far using Bethe-Salpeter equation have failed.
- Equally pressing, some might say more so, is the three-quark problem; viz., baryons in **QCD**.
 - Understanding that problem will help in making predictions for exotics



Grand Unification

Craig Roberts: Bound state problem in continuum QCD (87p)

Sao Paulo: II Workshop on Perspectives in
Nonperturbative QCD, 12-13 May 14



Unification of Meson & Baryon Properties

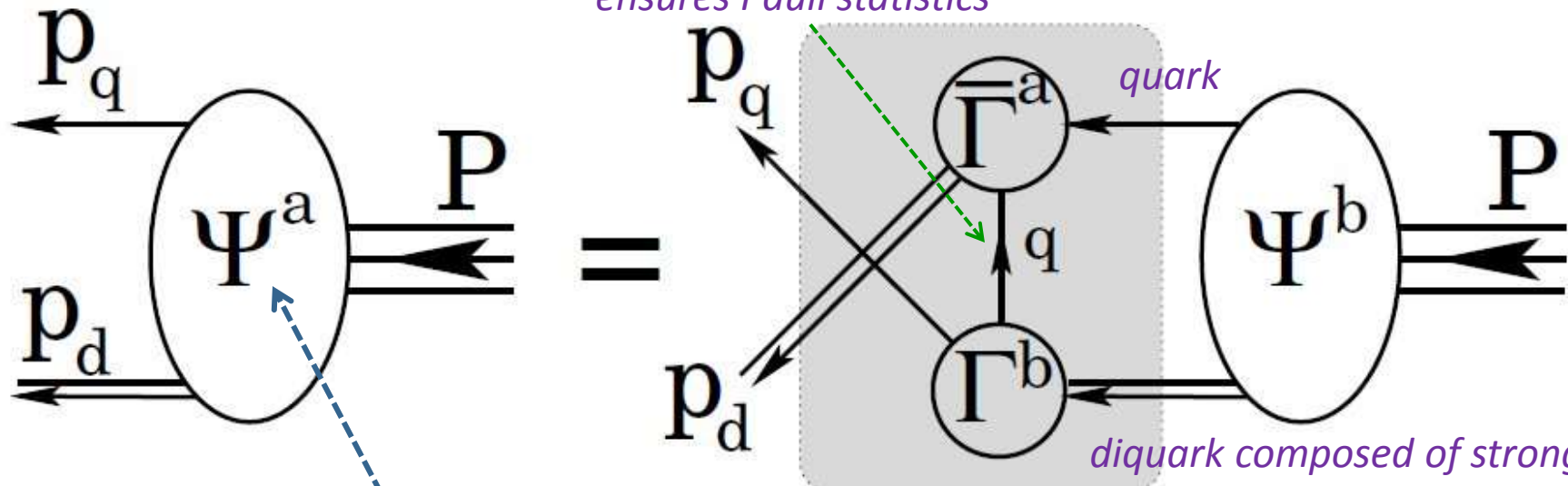
- Correlate the properties of meson and baryon ground- and excited-states within a *single, symmetry-preserving framework*
 - Symmetry-preserving means:
Poincaré-covariant & satisfy relevant Ward-Takahashi identities
- Constituent-quark model has hitherto been the most widely applied spectroscopic tool; whilst its weaknesses are emphasized by critics and acknowledged by proponents, it is of continuing value because there is nothing better that is yet providing a bigger picture.
- Nevertheless,
 - no connection with quantum field theory & therefore not with **QCD**
 - not symmetry-preserving & therefore cannot veraciously connect meson and baryon properties

DSEs & Baryons

- *Dynamical chiral symmetry breaking* (DCSB)
 - has enormous impact on meson properties.
 - *Must be included in description and prediction of baryon properties.*
- DCSB is essentially a quantum field theoretical effect.
In quantum field theory
 - Meson appears as pole in four-point quark-antiquark Green function
→ Bethe-Salpeter Equation
 - *Nucleon appears as a pole in a six-point quark Green function*
→ Faddeev Equation.
- Poincaré covariant Faddeev equation sums all possible exchanges and interactions that can take place between three dressed-quarks
- Tractable equation is based on the observation that an interaction which describes colour-singlet mesons also generates *nonpointlike* quark-quark (**diquark**) correlations in the colour-antitriplet channel

$$\text{SU}_c(3): 3 \otimes 3 = \bar{3} \oplus 6$$

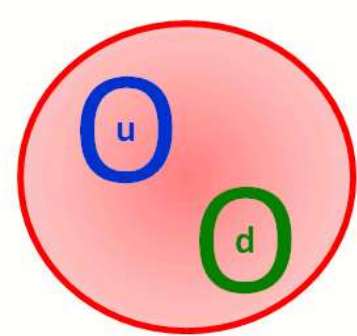
Faddeev Equation



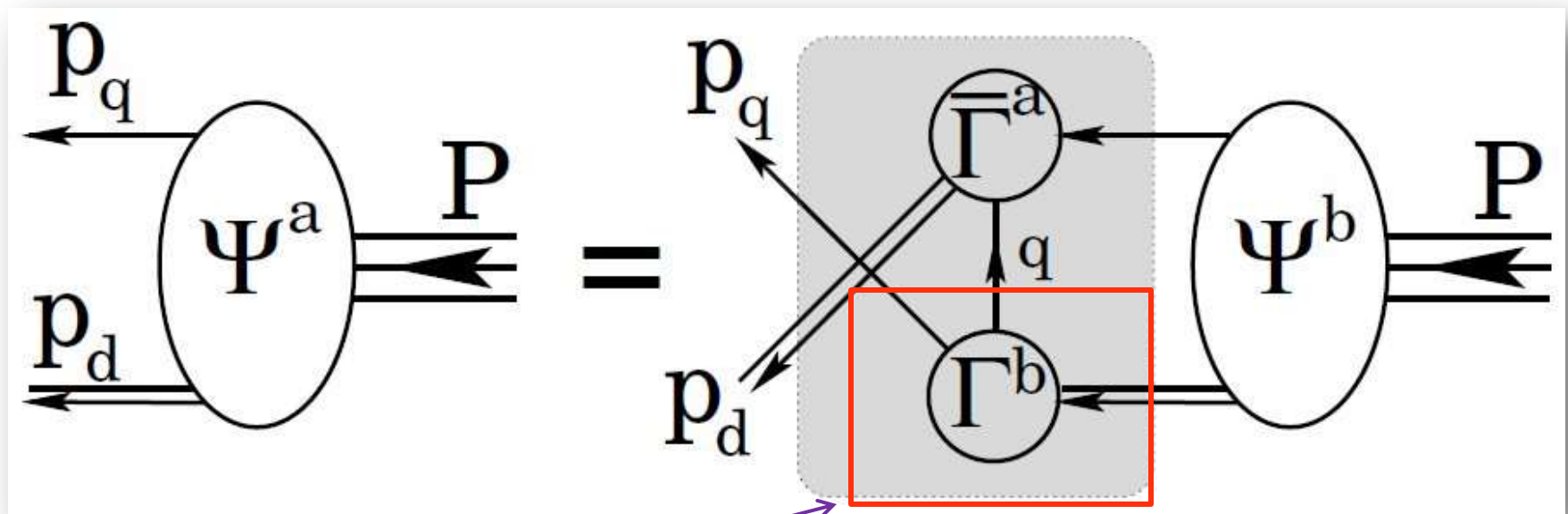
- Linear, Homogeneous Matrix equation
 - ❖ Yields *wave function (Poincaré Covariant Faddeev Amplitude)* that describes quark-diquark relative motion within the nucleon
- Scalar and Axial-Vector Diquarks . .
 - ❖ Both have “*correct*” parity and “*right*” masses
 - ❖ In Nucleon’s Rest Frame Amplitude has *s-, p- & d-wave correlations*

S-wave contributes only 37% to normalisation of wave function

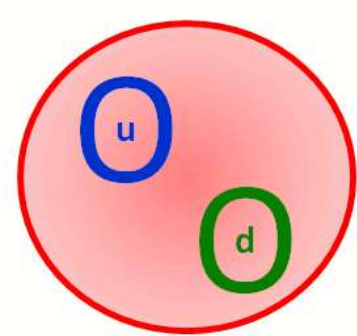
Faddeev Equation



- Why should a pole approximation produce reliable results?



quark-quark scattering matrix
- a pole approximation is used to arrive at the Faddeev-equation



Calculation of diquark masses in QCD

R.T. Cahill, C.D. Roberts and J. Praschifka

[Phys.Rev. D36 \(1987\) 2804](#)

Diquarks

Consider the rainbow-gap and ladder-Bethe-Salpeter equations

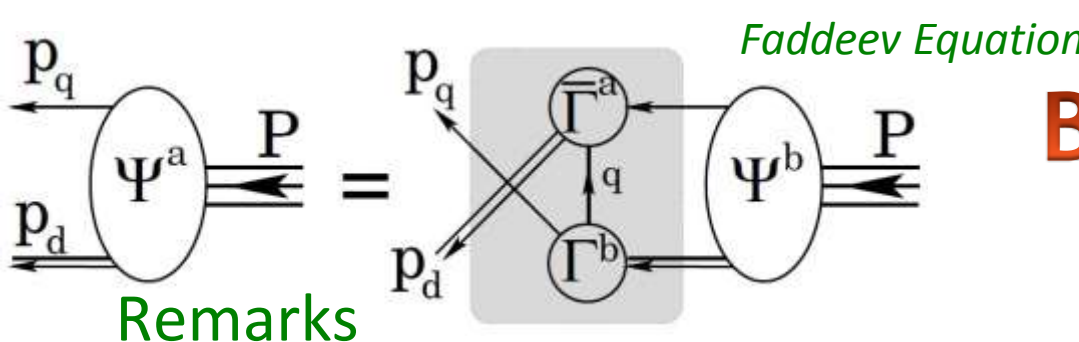
$$S(p)^{-1} = i\gamma \cdot p + m + \int \frac{d^4 q}{(2\pi)^4} g^2 D_{\mu\nu}(p-q) \frac{\lambda^a}{2} \gamma_\mu S(q) \frac{\lambda^a}{2} \gamma_\nu (q, p),$$

$$\Gamma(k; P) = - \int \frac{d^4 q}{(2\pi)^4} g^2 D_{\mu\nu}(p-q) \frac{\lambda^a}{2} \gamma_\mu S(q+P) \Gamma(q; P) S(q) \frac{\lambda^a}{2} \gamma_\nu.$$

- In this symmetry-preserving truncation, colour-antitriplet quark-quark correlations (diquarks) are described by a very similar homogeneous Bethe-Salpeter equation

$$\Gamma_{qq}(k; P) C^\dagger = - \frac{1}{2} \int \frac{d^4 q}{(2\pi)^4} g^2 D_{\mu\nu}(p-q) \frac{\lambda^a}{2} \gamma_\mu S(q+P) \Gamma_{qq}(q; P) C^\dagger S(q) \frac{\lambda^a}{2} \gamma_\nu$$

- Only difference is factor of $\frac{1}{2}$
- Hence, an interaction that describes mesons also generates diquark correlations in the colour-antitriplet channel



Baryon Structure

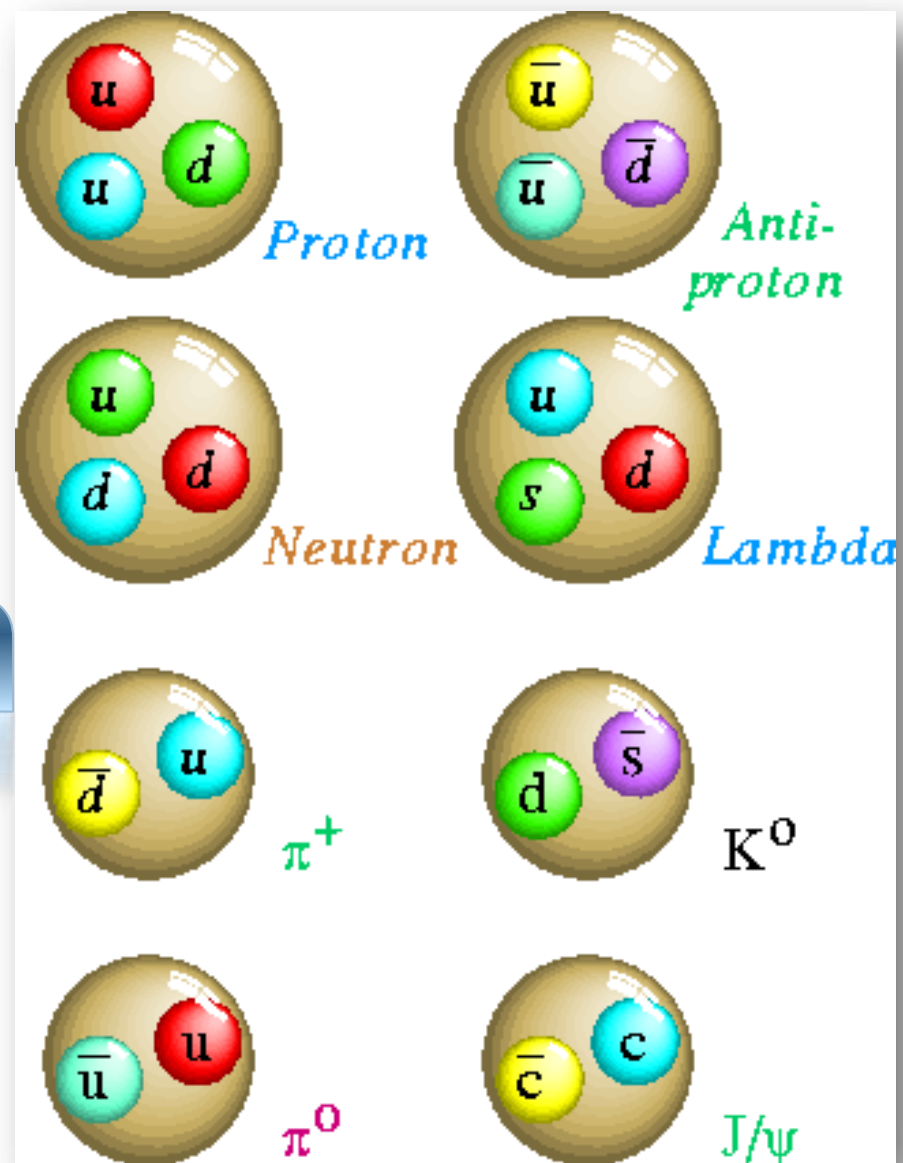
$SU(2)$ isospin symmetry of hadrons might emerge from mixing half-integer spin particles with their antiparticles.

- Diquark correlations are *not* inserted by hand

Such correlations are a dynamical consequence of strong-coupling in **QCD**

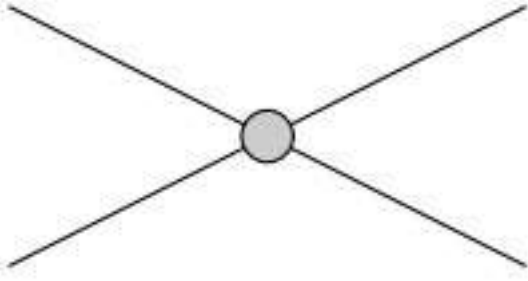
- The same mechanism that produces an almost massless pion from two dynamically-massive quarks;
i.e., DCSB, forces a strong correlation between two quarks in colour-antitriplet channels within a baryon
 - an indirect consequence of Pauli-Gürsey symmetry
- Diquark correlations are electromagnetically active and non-pointlike
 - Typically, $r_{0+} \sim r_\pi$ & $r_{1+} \sim r_\rho$ (actually 10% larger)
 - They have soft form factors

Baryon Spectrum



Motivation

- One method by which to validate QCD is computation of its hadron spectrum and subsequent comparison with modern experiment. Indeed, this is an integral part of the international effort in nuclear physics.
- For example, the N^* programme and the search for hybrid and exotic mesons together address the questions:
 - which hadron states and resonances are produced by QCD?
 - how are they constituted?
- This intense effort in hadron spectroscopy is a motivation to extend the research just described and treat ground- and excited-state hadrons with s -quark content. (New experiments planned in Japan)
- Key elements in a successful spectrum computation are:
 - symmetries and the pattern by which they are broken;
 - the mass-scale associated with confinement and DCSB;
 - and full knowledge of the physical content of bound-state kernels.All this is provided by the DSE approach.



Contact-Interaction Kernel

- Vector-vector contact interaction

$$g^2 D_{\mu\nu}(p - q) = \delta_{\mu\nu} \frac{4\pi\alpha_{\text{IR}}}{m_G^2}$$

$m_G = 800\text{MeV}$ is a gluon mass-scale

– dynamically generated in **QCD**

- Gap equation: $M_f = m_f + M_f \frac{4\alpha_{\text{IR}}}{3\pi m_G^2} \int_0^\infty ds s \frac{1}{s + M_f^2}$

➤ DCSB: $M \neq 0$ is possible so long as $\alpha_{\text{IR}} > \alpha_{\text{IR}}^{\text{critical}} = 0.4\pi$

➤ Observables require $\alpha_{\text{IR}} = 0.93\pi$



Contact Interaction

➤ Symmetry-preserving treatment of vector×vector contact interaction is useful tool for the study of phenomena characterised by probe momenta less-than the dressed-quark mass, M .

Because: *For experimental observables determined by probe momenta $Q^2 < M^2$, contact interaction results are not realistically distinguishable from those produced by the most sophisticated renormalisation-group-improved kernels.*

- Symmetry-preserving regularisation of the contact interaction serves as a useful surrogate, opening domains which analyses using interactions that more closely resemble those of QCD are as yet unable to enter.
- They're critical in attempts to use data as tool for charting nature of the quark-quark interaction at long-range; i.e., identifying signals of the running of couplings and masses in QCD.

Symmetry-preserving treatment of vector-vector contact-interaction: series of papers establishes strengths & limitations.

Contact Interaction

- [arXiv:1212.2212 \[nucl-th\]](https://arxiv.org/abs/1212.2212), Phys. Rev. C **87** 92013) 045207 [15 pages]
Features and flaws of a contact interaction treatment of the kaon
Chen Chen, L. Chang, C. D. Roberts, S. M. Schmidt, Shaolong Wan and D. J. Wilson,
- [arXiv:1209.4352 \[nucl-th\]](https://arxiv.org/abs/1209.4352), Phys. Rev. C**87** (2013) 015205 [12 pages]
Electric dipole moment of the rho-meson
M. Pitschmann, C.-Y. Seng, M. J. Ramsey-Musolf, C. D. Roberts, S. M. Schmidt and D. J. Wilson
- [arXiv:1204.2553 \[nucl-th\]](https://arxiv.org/abs/1204.2553), Few Body Syst. (2012) DOI: 10.1007/s00601-012-0466-3
Spectrum of Hadrons with Strangeness,
Chen Chen, L. Chang, C.D. Roberts, Shaolong Wan and D.J. Wilson
- [arXiv:1112.2212 \[nucl-th\]](https://arxiv.org/abs/1112.2212), Phys. Rev. C**85** (2012) 025205 [21 pages]
Nucleon and Roper electromagnetic elastic and transition form factors,
D. J. Wilson, I. C. Cloët, L. Chang and C. D. Roberts
- [arXiv:1102.4376 \[nucl-th\]](https://arxiv.org/abs/1102.4376), Phys. Rev. C **83**, 065206 (2011) [12 pages],
 π - and p -mesons, and their diquark partners, from a contact interaction,
H.L.L. Roberts, A. Bashir, L.X. Gutiérrez-Guerrero, C.D. Roberts and David J. Wilson
- [arXiv:1101.4244 \[nucl-th\]](https://arxiv.org/abs/1101.4244), Few Body Syst. **51** (2011) pp. 1-25
Masses of ground and excited-state hadrons
H.L.L. Roberts, Lei Chang, Ian C. Cloët and Craig D. Roberts
- [arXiv:1009.0067 \[nucl-th\]](https://arxiv.org/abs/1009.0067), Phys. Rev. C**82** (2010) 065202 [10 pages]
Abelian anomaly and neutral pion production
Hannes L.L. Roberts, C.D. Roberts, A. Bashir, L. X. Gutiérrez-Guerrero & P. C. Tandy
- [arXiv:1002.1968 \[nucl-th\]](https://arxiv.org/abs/1002.1968), Phys. Rev. C **81** (2010) 065202 (5 pages)
Pion form factor from a contact interaction, L. Xiomara Gutiérrez-Guerrero, A. Bashir, I. C. Cloët & C. D. Roberts

Craig Roberts: Bound state problem in continuum QCD (87p)

Sao Paulo: II Workshop on Perspectives in
Nonperturbative QCD, 12-13 May 14

Spectrum of Hadrons with Strangeness

- Solve gap equation for u & s -quarks

Table 1 Computed dressed-quark properties, required as input for the Bethe-Salpeter and Faddeev equations, and computed values for in-hadron condensates [52; 53; 54]. All results obtained with $\alpha_{\text{IR}} = 0.93\pi$ and (in GeV) $\Lambda_{\text{ir}} = 0.24$, $\Lambda_{\text{uv}} = 0.905$. N.B. These parameters take the values determined in the spectrum calculation of Ref. [6]; and we assume isospin symmetry throughout. (All dimensioned quantities are listed in GeV.)

m_u	m_s	m_s/m_u	M_0	M_u	M_s	M_s/M_u	$\kappa_0^{1/3}$	$\kappa_\pi^{1/3}$	$\kappa_K^{1/3}$
0.007	0.17	24.3	0.36	0.37	0.53	1.43	0.241	0.243	0.246

- Input ratio $m_s/m_u = 24$ is consistent with modern estimates
- Output ratio $M_s/M_u = 1.43$ shows dramatic impact of DCSB, even on the s -quark: $M_s - m_s = 0.36 \text{ GeV} = M_0$
 - ... This is typical of all DSE and lattice studies
- $\kappa = \text{in-hadron condensate}$ rises slowly with mass of hadron

Spectrum of Mesons with Strangeness

- Solve Bethe-Salpeter equations for **mesons** and diquarks

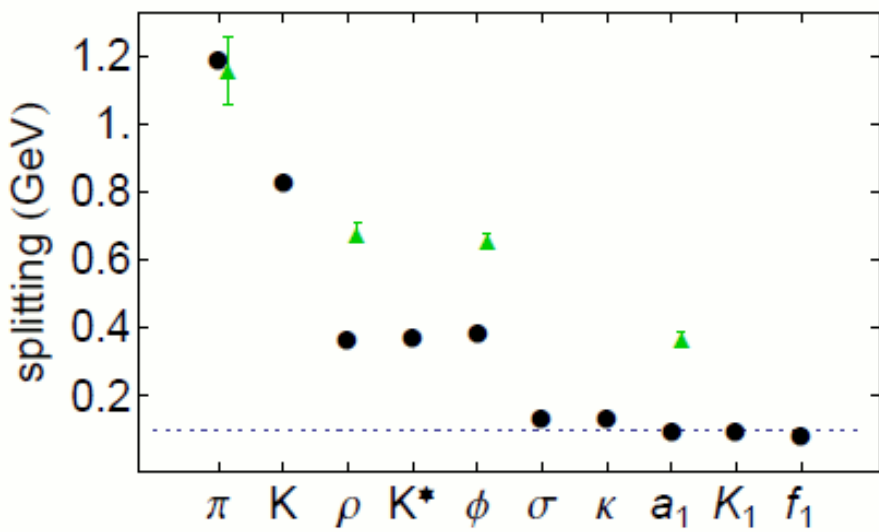
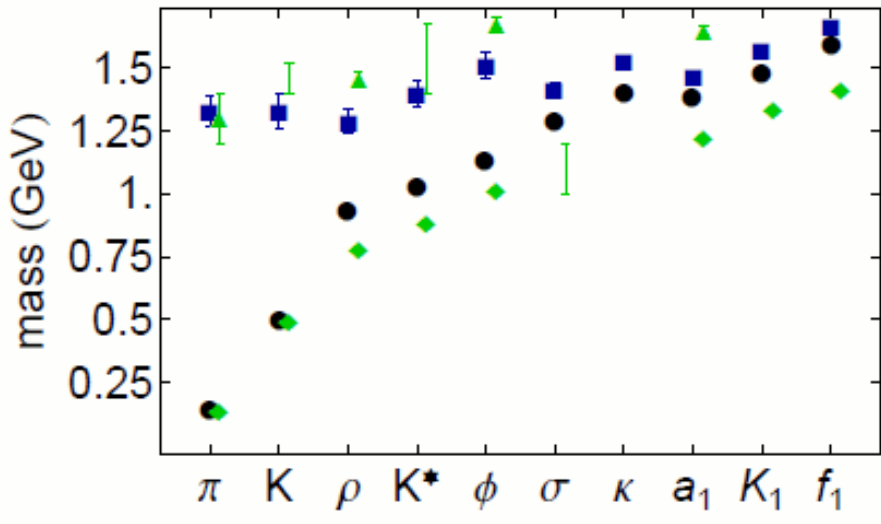
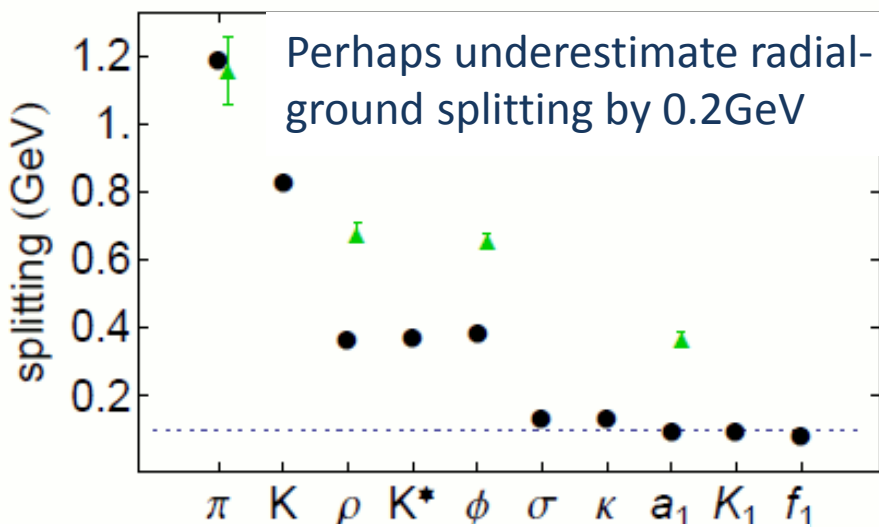
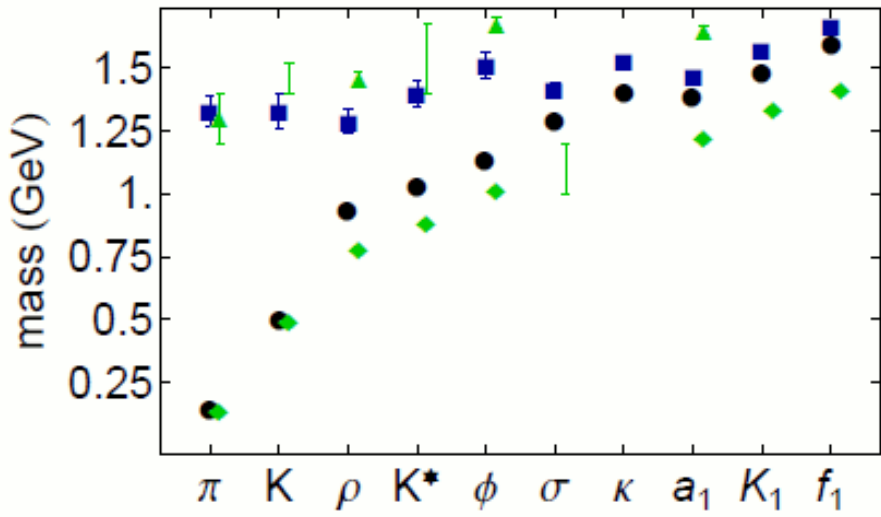


Fig. 2 Left panel: Pictorial representation of Table 2. *Circles* – computed ground-state masses; *squares* – computed masses of radial excitations; *diamonds* – empirical ground-state masses in Row 2; and *triangles* – empirical radial excitation masses in Row 4. Right panel: *Circles* – computed splitting between the first radial excitation and ground state in each channel; and *triangles* – empirical splittings, where they are known. The *dashed line* marks a splitting of 0.1 GeV.

Spectrum of Mesons with Strangeness

- Solve Bethe-Salpeter equations for **mesons** and diquarks



- ✓ Computed values for ground-states are greater than the empirical masses, where they are known.
- ✓ Typical of DCSB-corrected kernels that omit resonant contributions; i.e., do not contain effects that may phenomenologically be associated with a meson cloud.



Fig. 2
comput
empiric
excitat
dashed

res –
les –
adial
The

Spectrum of Diquarks with Strangeness

- Solve Bethe-Salpeter equations for mesons and **diquarks**

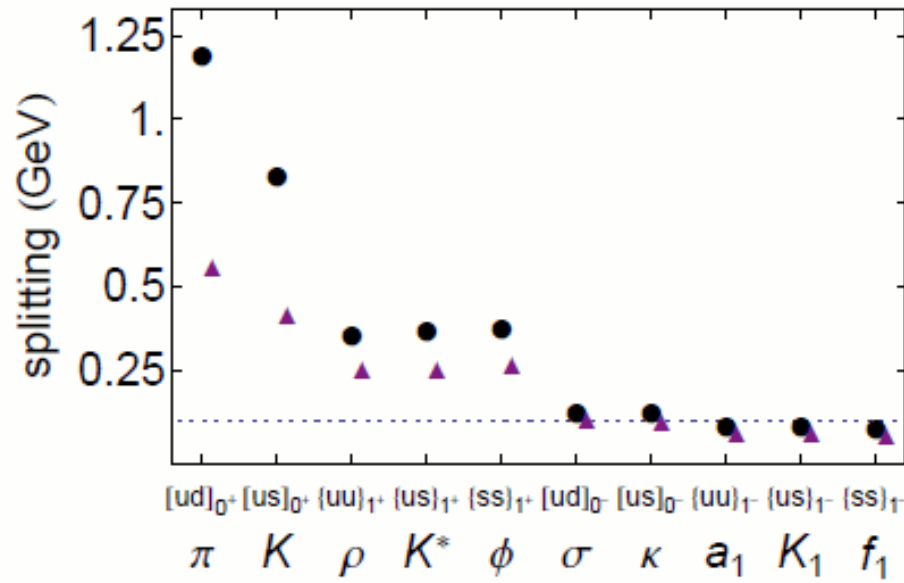
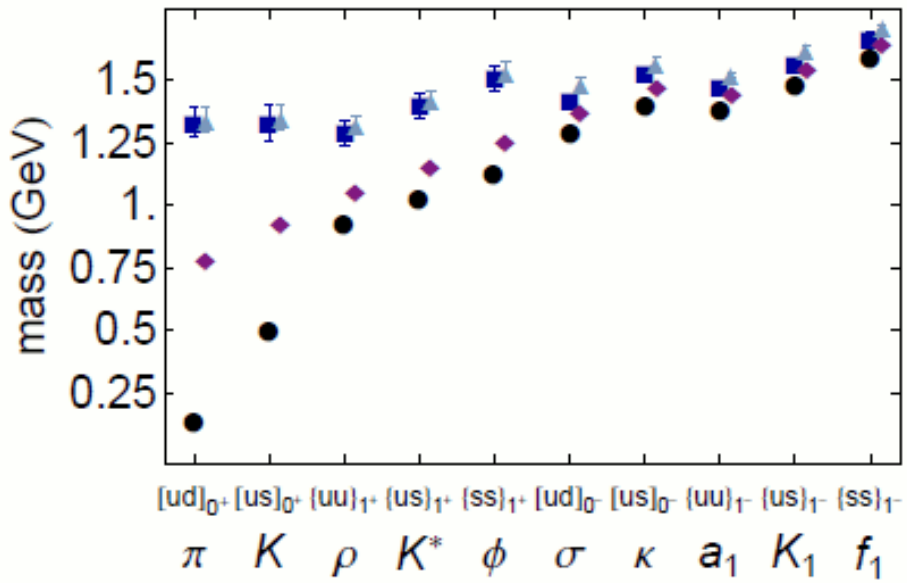
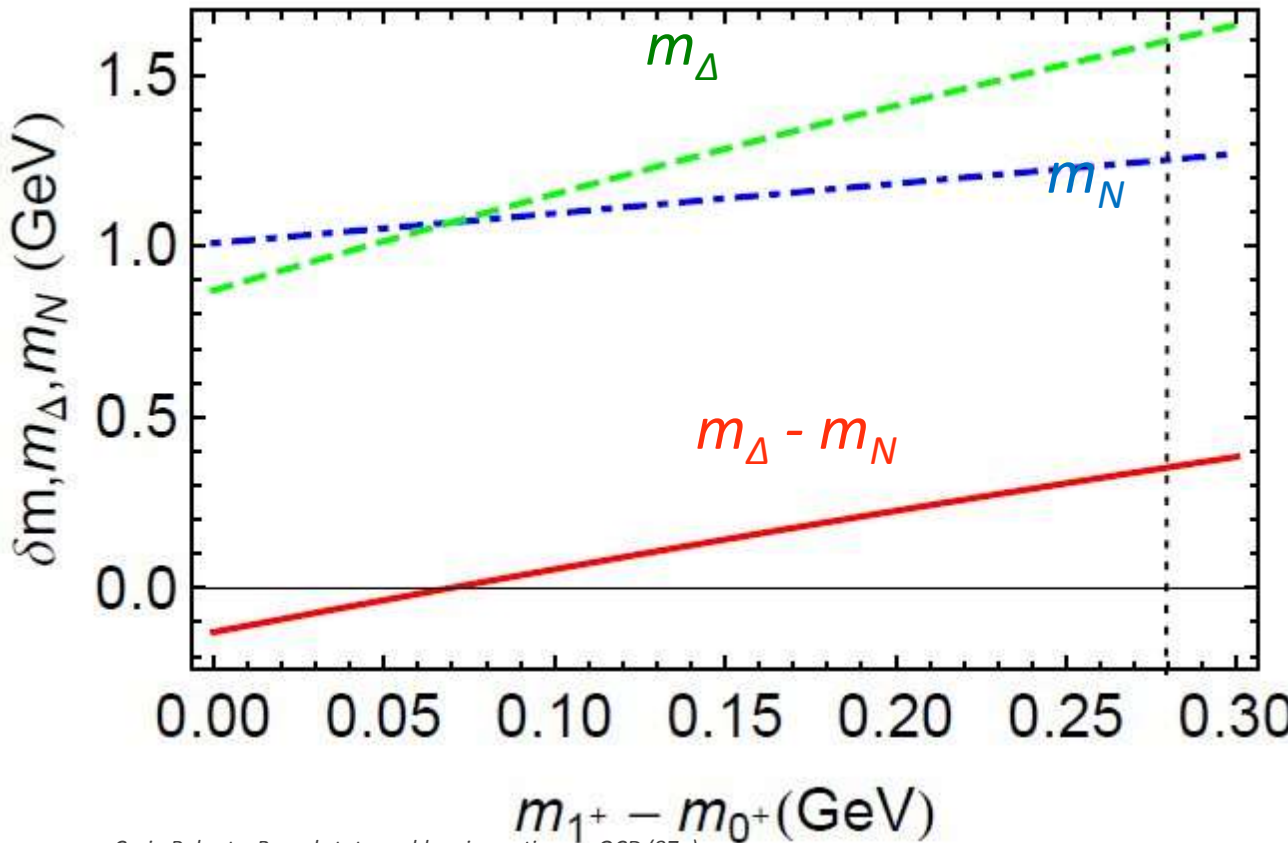


Fig. 3 Left panel: Pictorial representation of Table 4. *Diamonds* – ground-state diquark masses in Row 1; *circles* – ground-state meson masses in Row 2; *triangles* – masses of diquark first radial excitations in Row 3; and *squares* – masses of meson radial excitations in Row 4. Right panel: *Diamonds* – for diquarks, computed splittings between first radial excitation and ground state; and *circles* – for mesons, computed splitting between the first radial excitation and ground state in each channel. The *dashed line* marks a splitting of 0.1 GeV.

Baryons & diquarks

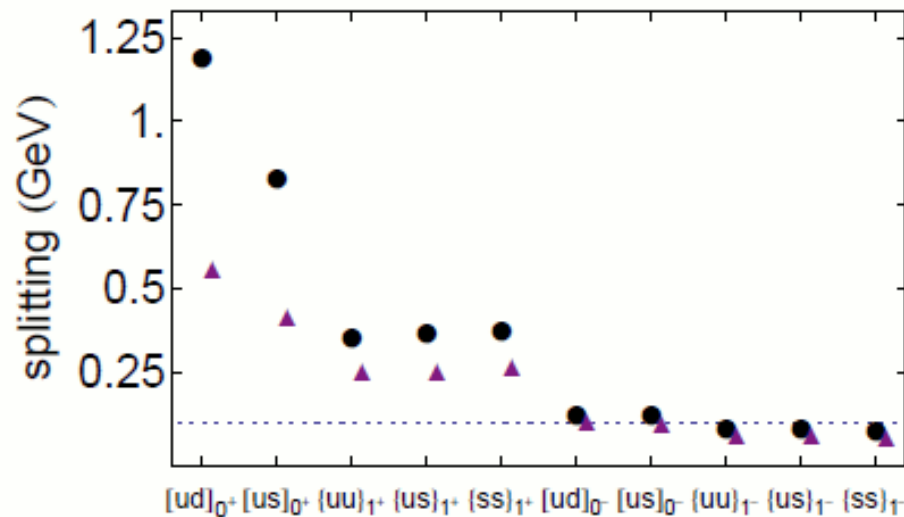
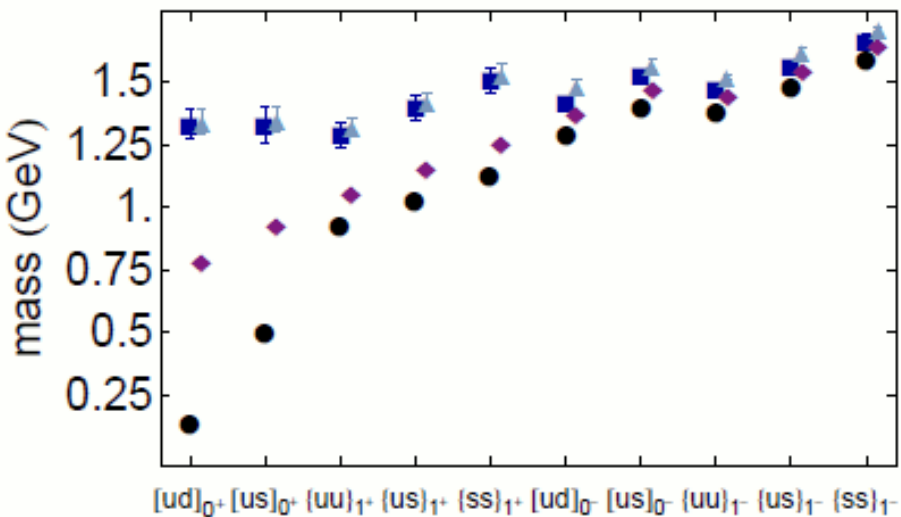
- From apparently simple material, one arrives at a powerful elucidative tool, which provides numerous insights into baryon structure; e.g.,
 - *There is a causal connection between $m_\Delta - m_N$ & $m_{1+} - m_{0+}$*



Physical splitting grows rapidly with increasing diquark mass difference

Spectrum of Diquarks with Strangeness

- Solve Bethe-Salpeter equations for mesons and **diquarks**



- ✓ Level ordering of diquark correlations is same as that for mesons.
- ✓ In all diquark channels, except scalar, mass of diquark's partner meson is a fair guide to the diquark's mass:
 - Meson mass bounds the diquark's mass from below;
 - Splitting always less than 0.13GeV and decreases with increasing meson mass
- ✓ Scalar channel “special” owing to DCSB

1 f_1

low 1;
low 3;
computed
between
V.

Fig. 3
circles -
and squ-
splitting
the first

Bethe-Salpeter amplitudes

- Bethe-Salpeter amplitudes are couplings in Faddeev Equation

Table 3 The structure of meson Bethe-Salpeter amplitudes is described in Sect. 2.2.1 and App. B. Here we list the canonically normalised amplitude associated with each of the BSE eigenstates in Table 2. Only pseudoscalar mesons involve two independent amplitudes when a vector \times vector contact interaction is treated systematically in rainbow-ladder truncation.

		m_π	m_K	m_ρ	m_{K^*}	m_ϕ	m_σ	m_κ	m_{a_1}	m_{K_1}	m_{f_1}
n=0	$E_{q\bar{q}}$	3.60	3.86	1.53	1.62	1.74	0.47	0.47	0.31	0.31	0.31
	$F_{q\bar{q}}$	0.48	0.60								
n=1	$E_{q\bar{q}}$	0.83	0.76	0.72	0.70	0.66	0.34	0.35	0.28	0.28	0.28
	$F_{q\bar{q}}$	0.05	1.18								

- Magnitudes for diquarks follow precisely the meson pattern

Table 5 The structure of diquark Bethe-Salpeter amplitudes is described in Sect. 2.2.2 and App. B. Here we list all canonically normalised amplitudes that are relevant to the baryons we consider. Only scalar diquarks involve two independent amplitudes.

	$ u, d _{0+}$	$ s, u _{0+}$	$\{u, u\}_{1+}$	$\{s, u\}_{1+}$	$\{s, s\}_{1+}$	$ u, d _{0-}$	$ s, u _{0-}$	$\{u, u\}_{1-}$	$\{s, u\}_{1-}$	$\{s, s\}_{1-}$
E_{qq}	2.74	2.91	1.30	1.36	1.42	0.40	0.39	0.27	0.27	0.26
F_{qq}	0.31	0.40								

Owing to DCSB, FE couplings in $\frac{1}{2}^-$ channels
are 25-times weaker than in $\frac{1}{2}^+$!

Spectrum of Baryons with Strangeness

- Solved all Faddeev equations, obtained masses and eigenvectors of the octet and decuplet baryons.

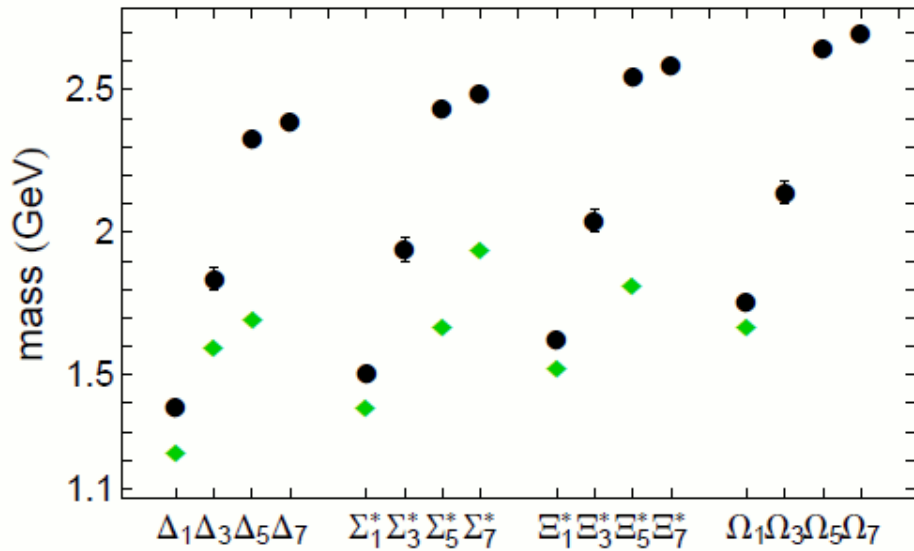
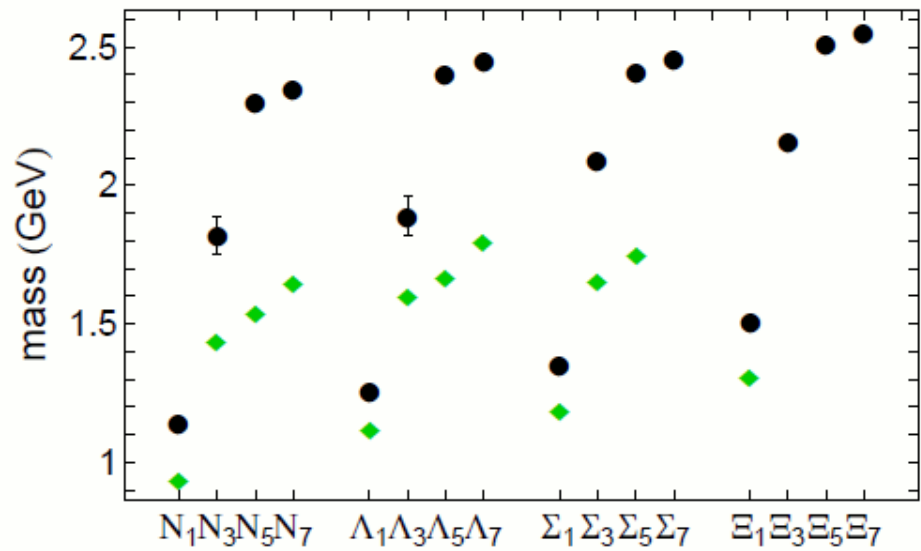


Fig. 4 Left panel: Pictorial representation of octet masses in Table 6. Circles – computed masses; and diamonds – empirical masses. On the horizontal axis we list a particle name with a subscript that indicates its row in the table; e.g., N_1 means nucleon column, row 1. In this way the labels step through ground-state, radial excitation, parity partner, parity partner's radial excitation. Right panel: Analogous plot for the decuplet masses in Table 6.

Spectrum of Baryons with Strangeness

- Comparison with bare masses from ANL-Osaka Coupled Channels Collaboration

Searched for best fit, including $(CC_{\text{BARE}} - \text{DSE})^2$

ANL-Osaka bare masses provide excellent description of enormous amount of data

	P_{11}	S_{11}	S_{11}	P_{33}	P_{33}	D_{33}
ANL-Osaka	1.83	2.04	2.61	1.28	2.16	2.13
DSE	1.83	2.30	2.35	1.39	1.84	2.33
Rel. Err.	0	11.3%	11.1%	7.9%	17.4%	8.6%

- rms |Rel. Err.| = $9.4 \pm 5.7 \%$

This is remarkable, given that the DSE results have neither been optimised nor tuned in any way.

Structure of Baryons with Strangeness

➤ Baryon structure is flavour-blind

Table 7 Contact interaction Faddeev amplitudes for each of the octet baryons and their low-lying excitations. The superscript in the expression s^i or a^i is a diquark enumeration label associated with Eq. (31), except for [2, 3] and [6, 8], which are the $I = 0$ combinations in Eq. (49).

Diquark content

		s^1	s^2	$s^{[2,3]}$	a_1^4	a_2^4	a_1^5	a_2^5	a_1^6	a_2^6	$a_1^{[6,8]}$	$a_2^{[6,8]}$	a_1^9	a_2^9	$P_{J=0}$
$(P = +, n = 0)$	N	0.88			-0.38	0.27	-0.06	0.04							78%
	Λ	0.67		-0.27								-0.45	-0.09		79%
	Σ		0.85		-0.45	0.26			0.12	0.02					72%
	Ξ		0.91		0.14	0.08							0.39	0.00	82%
$(P = +, n = 1)$	N	-0.02			0.52	-0.37	-0.63	0.44							0%
	Λ	0.03		0.06								-0.78	0.63		0%
	Σ		0.00		-0.04	0.02			0.83	-0.55					0%
	Ξ		0.00		0.01	-1.00							-0.02	0.06	0%
$(P = -, n = 0)$	N	0.71			-0.41	0.29	0.41	-0.29							50%
	Λ	0.64		0.44								-0.47	0.42		61%
	Σ		0.61		-0.47	0.23			0.55	-0.21					38%
	Ξ		0.76		-0.34	0.35							0.33	-0.28	58%
$(P = -, n = 1)$	N	0.66			-0.41	0.29	0.45	-0.32							44%
	Λ	0.60		0.43								-0.48	0.47		55%
	Σ		0.57		-0.47	0.23			0.58	-0.24					33%
	Ξ		0.73		-0.34	0.37							0.33	-0.31	54%

➤ Baryon structure is flavour-blind

Structure of Baryons with Strangeness

Table 7 Contact interaction Faddeev amplitudes for each of the octet baryons and their low-lying excitations. The superscript in the expression s^i or a^i is a diquark enumeration label associated with Eq. (31), except for [2, 3] and [6, 8], which are the $I = 0$ combinations in Eq. (49).

Diquark content

		s^1	s^2	$s^{[2,3]}$	a_1^4	a_2^4	a_1^5	a_2^5	a_1^6	a_2^6	$a_1^{[6,8]}$	$a_2^{[6,8]}$	a_1^9	a_2^9	$P_{J=0}$
(P = +, n = 0)	N	➤ $J_{qq}=0$ content of $J=\frac{1}{2}$ baryons is almost independent of their flavour structure													78%
	Λ														79%
	Σ														72%
	Ξ														82%
(P = +, n = 1)	N	➤ <i>Radial excitation of ground-state octet possess zero scalar diquark content!</i>													0%
	Λ														0%
	Σ														0%
	Ξ														0%
(P = -, n = 0)	N	➤ <i>This is a consequence of DCSB</i>													50%
	Λ														61%
	Σ														38%
	Ξ														58%
(P = -, n = 1)	N	➤ <i>Ground-state (1/2)⁺ possess unnaturally large scalar diquark content</i>													44%
	Λ														55%
	Σ														33%
	Ξ														54%

Spectrum of Hadrons with Strangeness

- Solved all Faddeev equations, obtained masses and eigenvectors of the octet and decuplet baryons.

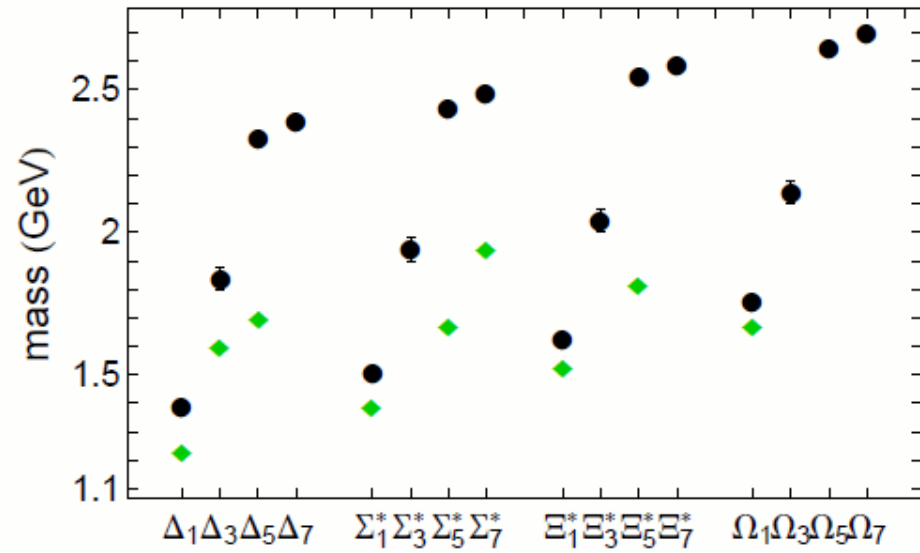
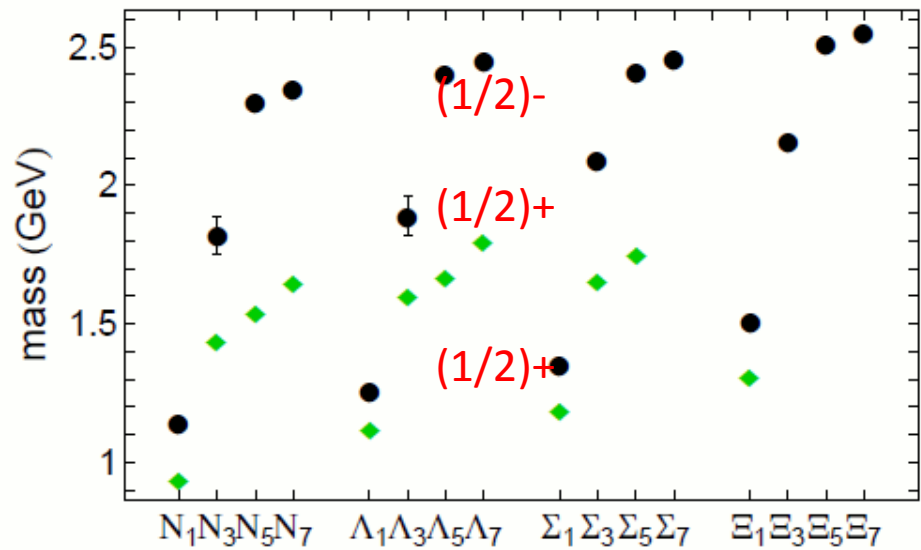


Fig. 4 Left panel: Pictorial representation of octet masses in Table 6. Circles – computed masses; and diamonds – empirical masses. On the horizontal axis we list a particle name with a subscript that indicates its row in the table; e.g., N_1 means nucleon column, row 1. In this way the labels step through ground-state, radial excitation, parity partner, parity partner's radial excitation. Right panel: Analogous plot for the decuplet masses in Table 6.

Spectrum of Hadrons with Strangeness

- Solved all Faddeev equations, obtained masses and eigenvectors of the octet and decuplet baryons.

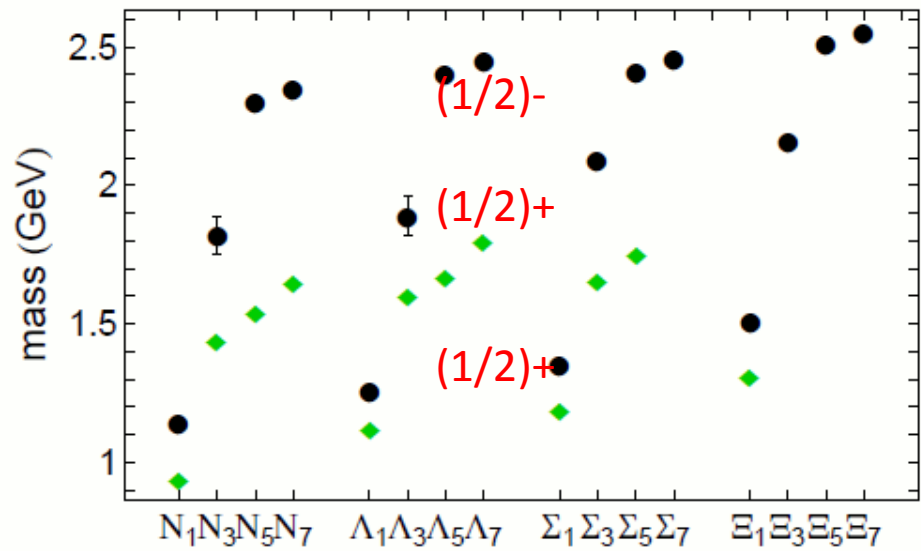
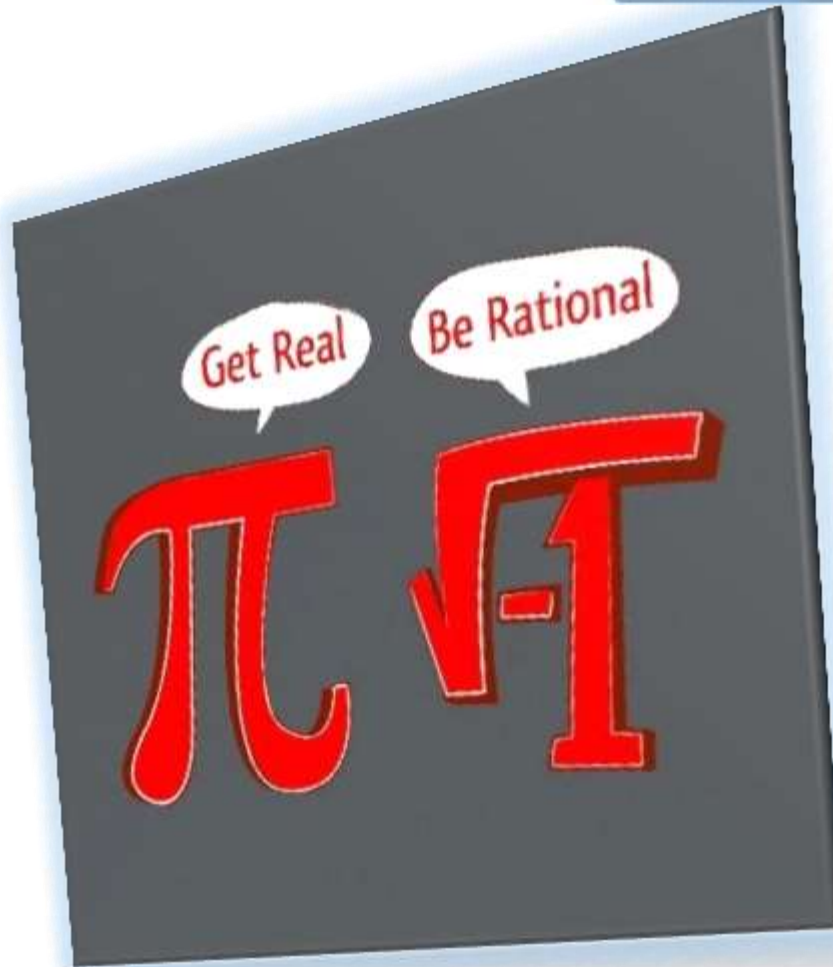


Fig. 4 Left panel: Pictorial representation of octet diamonds – empirical masses. On the horizontal axis its row in the table; e.g., N_1 means nucleon column, radial excitation, parity partner, parity partner's radial masses in Table 6.

- This level ordering has long been a problem in CQMs with linear or HO confinement potentials
- *Correct ordering owes to DCSB*
 - *Positive parity diquarks have Faddeev equation couplings 25-times greater than negative parity diquarks*
- Explains why approaches within which DCSB cannot be realised (CQMs) or simulations whose parameters suppress DCSB will both have difficulty reproducing experimental ordering



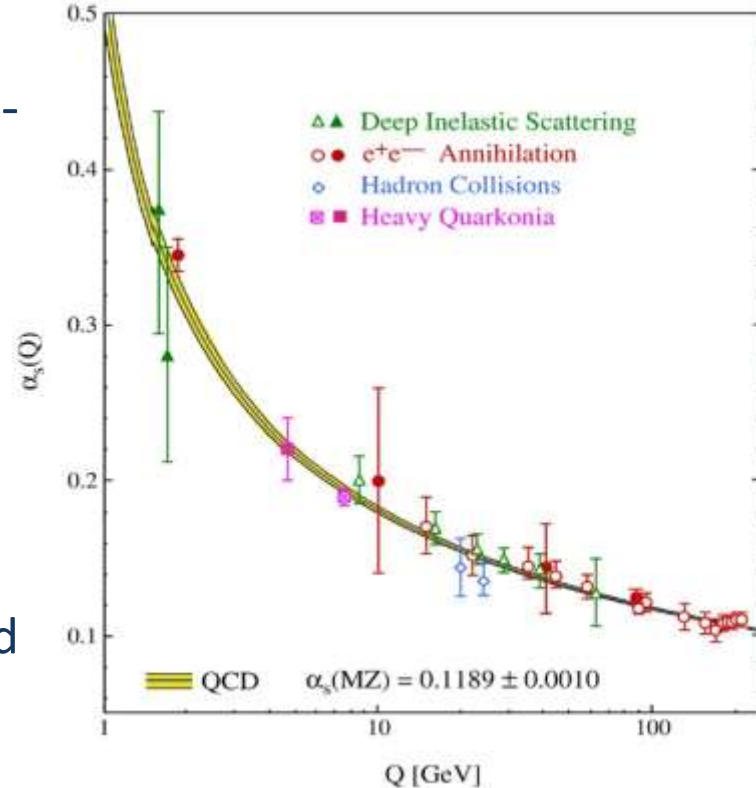
Getting real

Craig Roberts: Bound state problem in continuum QCD (87p)

Sao Paulo: II Workshop on Perspectives in
Nonperturbative QCD, 12-13 May 14

Charting the Interaction

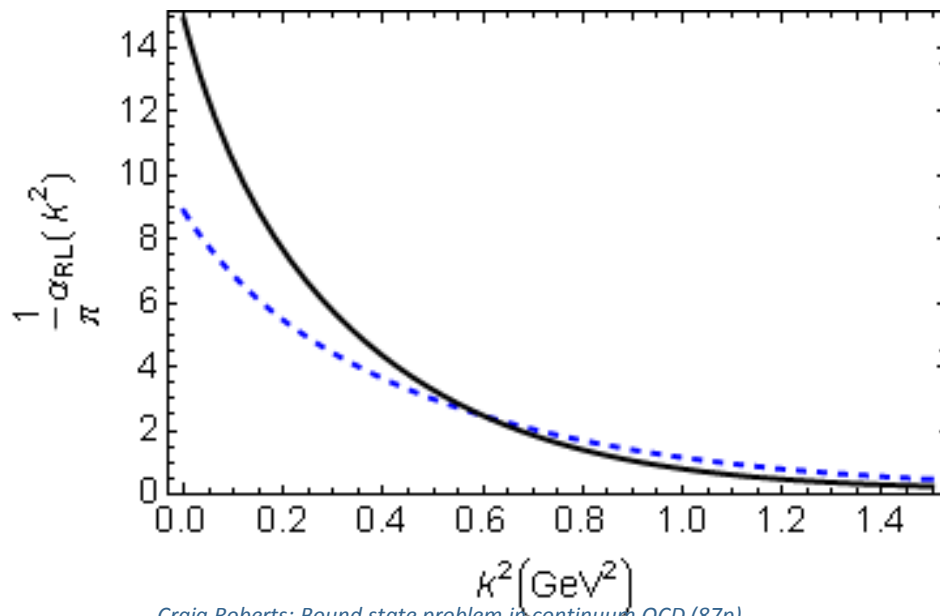
- Interaction in QCD is not momentum-independent
 - Behaviour for $Q^2 > 2\text{GeV}^2$ is well known; namely, renormalisation-group-improved one-gluon exchange
 - Computable in perturbation theory
- Known = there is a “freezing” of the interaction below a scale of roughly 0.4GeV , which is partly why momentum-independent interaction works
- Unknown
 - Infrared behavior of the interaction, which is responsible for
 - Confinement
 - DCSB
 - How is the transition to pQCD made and is it possible to define a transition boundary?



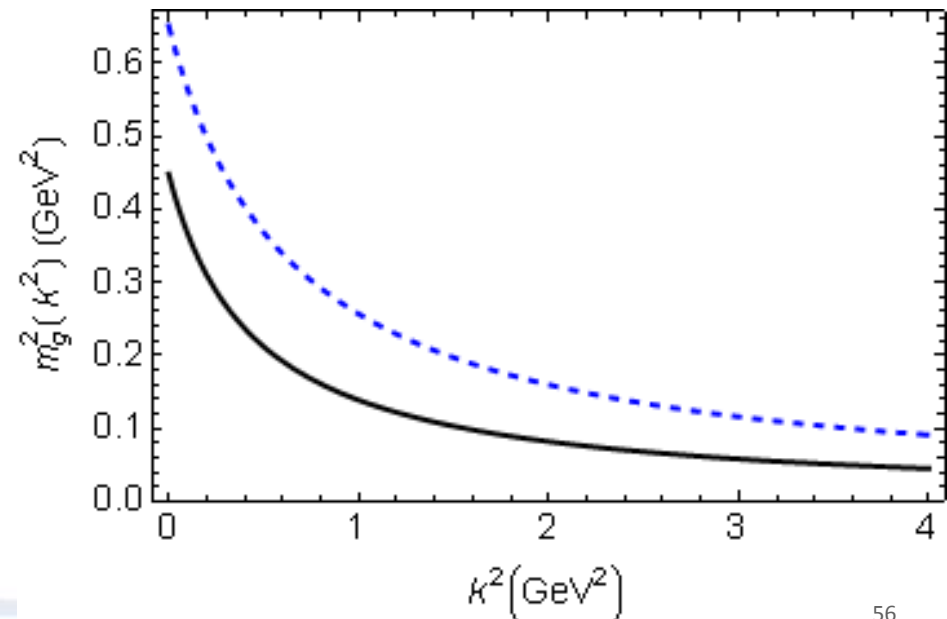
DSE Studies

- Phenomenology of gluon

- Wide-ranging study of π & ρ properties
- Effective coupling
 - Agrees with pQCD in ultraviolet
 - Saturates in infrared
 - $\alpha(0)/\pi = 8-15$
 - $\alpha(m_G^2)/\pi = 2-4$
- Running gluon mass
 - Gluon is massless in ultraviolet in agreement with pQCD
 - Massive in infrared
 - $m_G(0) = 0.67-0.81 \text{ GeV}$
 - $m_G(m_G^2) = 0.53-0.64 \text{ GeV}$



Craig Roberts: Bound state problem in continuum QCD (87p)

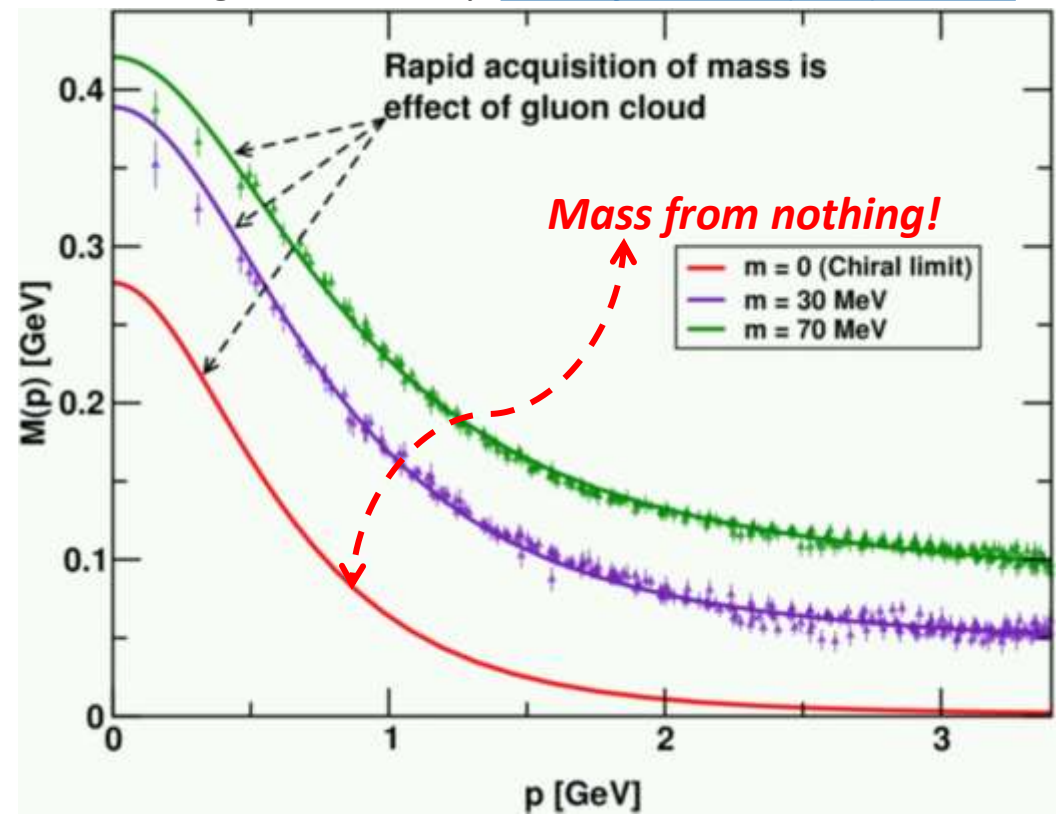


$$S(p) = \frac{Z(p^2)}{i\gamma \cdot p + M(p^2)}$$

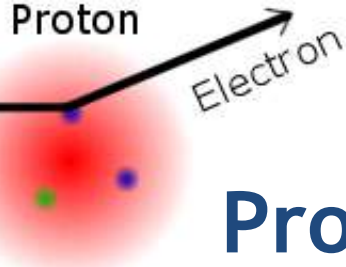
DCSB

C.D. Roberts, [Prog. Part. Nucl. Phys. 61 \(2008\) 50](#)

M. Bhagwat & P.C. Tandy, [AIP Conf. Proc. 842 \(2006\) 225-227](#)



- quark's mass depends on its momentum.
- Mass function can be calculated and is depicted here.
- Continuum- and Lattice-QCD are in agreement: the vast bulk of the light-quark mass comes from a cloud of gluons, dragged along by the quark as it propagates.



Nucleon Structure Probed in scattering experiments

- Electron is a good probe because it is structureless

Structureless fermion, or simply structured fermion, $F_1=1$ & $F_2=0$, so that $G_E=G_M$ and hence distribution of charge and magnetisation within this fermion are identical

- Proton's electromagnetic current

$$\begin{aligned} J_\mu(P', P) &= ie \bar{u}_p(P') \Lambda_\mu(Q, P) u_p(P), \\ &= ie \bar{u}_p(P') \left(\gamma_\mu F_1(Q^2) + \frac{1}{2M} \sigma_{\mu\nu} Q_\nu F_2(Q^2) \right) u_p(P) \end{aligned}$$

F_1 = Dirac form factor F_2 = Pauli form factor

$$G_E(Q^2) = F_1(Q^2) - \frac{Q^2}{4M^2} F_2(Q^2), \quad G_M(Q^2) = F_1(Q^2) + F_2(Q^2)$$

G_E = Sachs Electric form factor

If a nonrelativistic limit exists, this relates to the charge density

G_M = Sachs Magnetic form factor

If a nonrelativistic limit exists, this relates to the magnetisation density

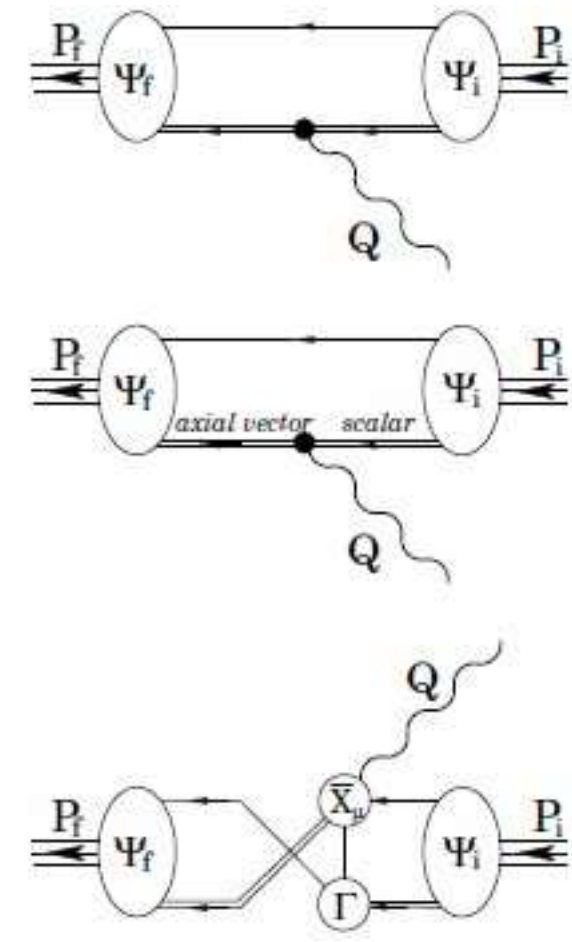
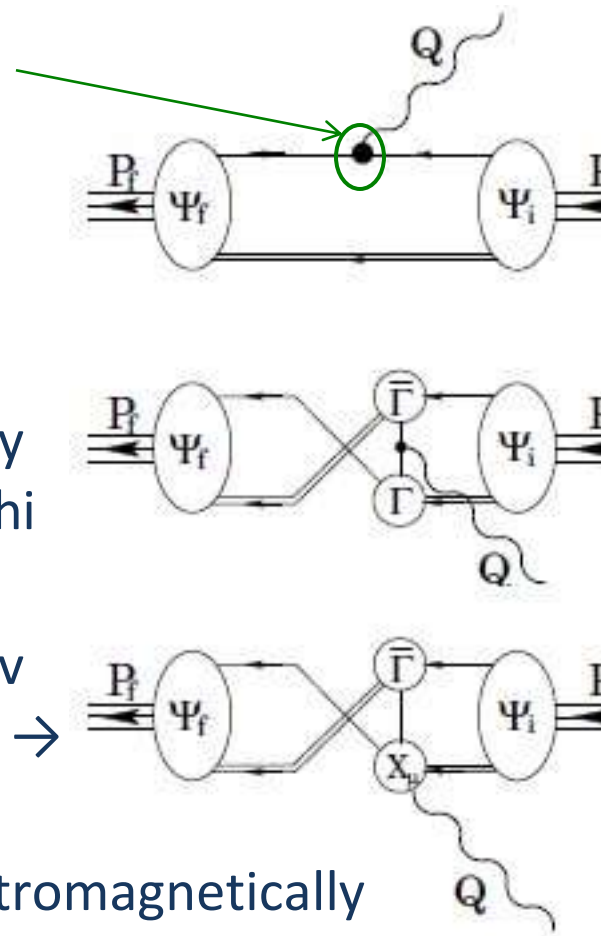
Nucleon form factors

- For the nucleon & Δ -resonance, studies of the Faddeev equation exist that are based on the 1-loop renormalisation-group-improved interaction that was used efficaciously in the study of mesons
 - *Toward unifying the description of meson and baryon properties*
G. Eichmann, I.C. Cloët, R. Alkofer, A. Krassnigg and C.D. Roberts
[arXiv:0810.1222 \[nucl-th\]](https://arxiv.org/abs/0810.1222), Phys. Rev. C **79** (2009) 012202(R) (5 pages)
 - *Survey of nucleon electromagnetic form factors*
I.C. Cloët, G. Eichmann, B. El-Bennich, T. Klähn and C.D. Roberts
[arXiv:0812.0416 \[nucl-th\]](https://arxiv.org/abs/0812.0416), Few Body Syst. **46** (2009) pp. 1-36
 - *Nucleon electromagnetic form factors from the Faddeev equation*
G. Eichmann, [arXiv:1104.4505 \[hep-ph\]](https://arxiv.org/abs/1104.4505)
- These studies retain the scalar and axial-vector diquark correlations, which we know to be necessary and sufficient for a reliable description
- In order to compute form factors, one needs a photon-nucleon current

Photon-nucleon current

Vertex must contain the dressed-quark anomalous magnetic moment

- Composite nucleon must interact with photon via nontrivial current constrained by Ward-Green-Takahashi identities
- DSE \rightarrow BSE \rightarrow Faddeev equation plus current \rightarrow nucleon form factors
- NB. Diquarks are electromagnetically active. Cannot ignore the photon-diquark coupling.



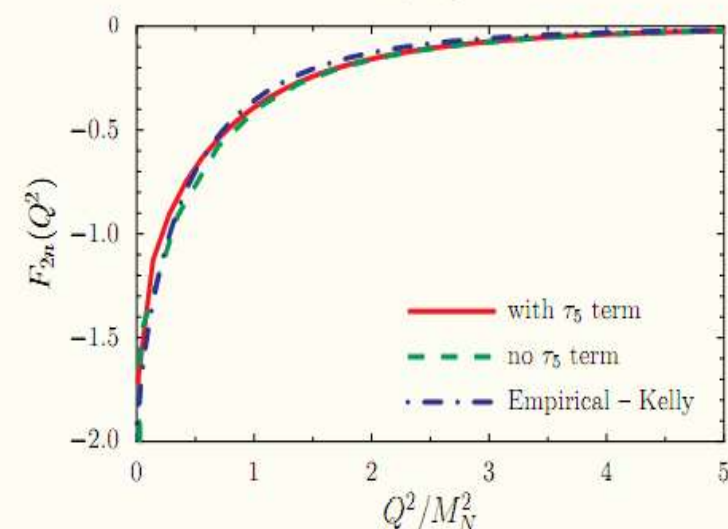
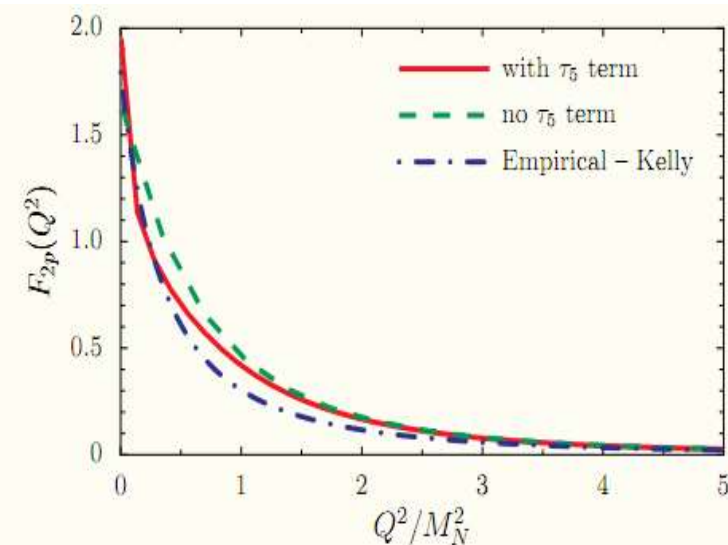
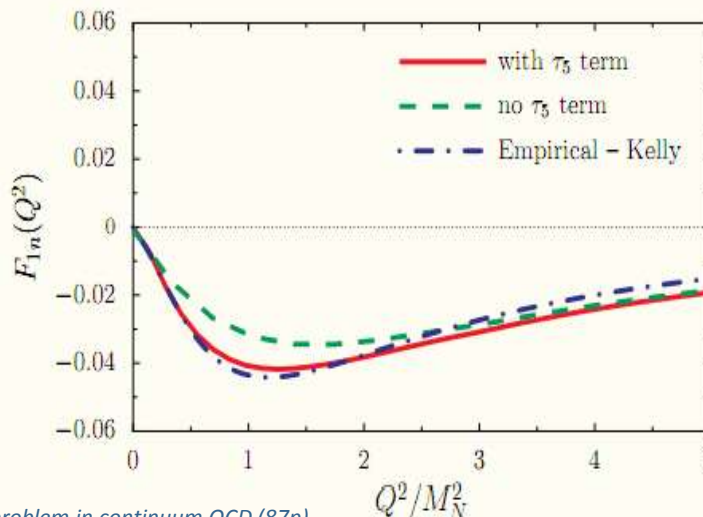
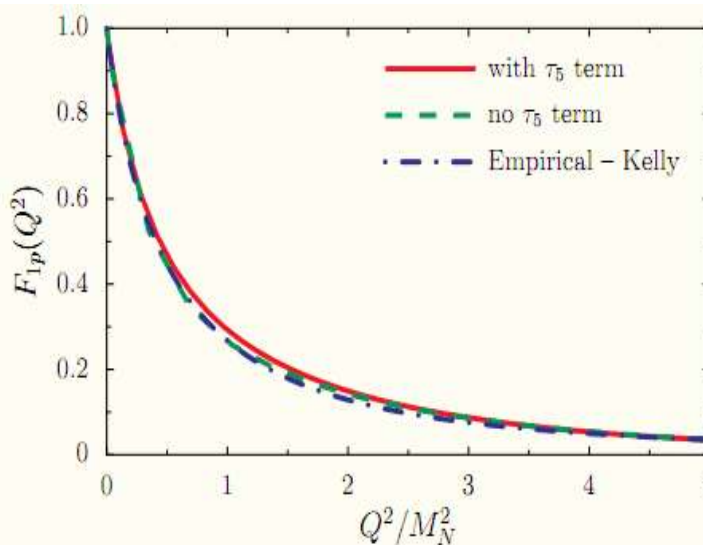
Oettel, Pichowsky, Smekal
[Eur.Phys.J. A8 \(2000\) 251-281](https://doi.org/10.1007/s100500000251)

Nucleon Form Factors

*Unification of meson
and nucleon form
factors.*

*Very good
description.*

*Quark's momentum-
dependent
anomalous magnetic
moment has
observable impact &
materially improves
agreement in all
cases.*

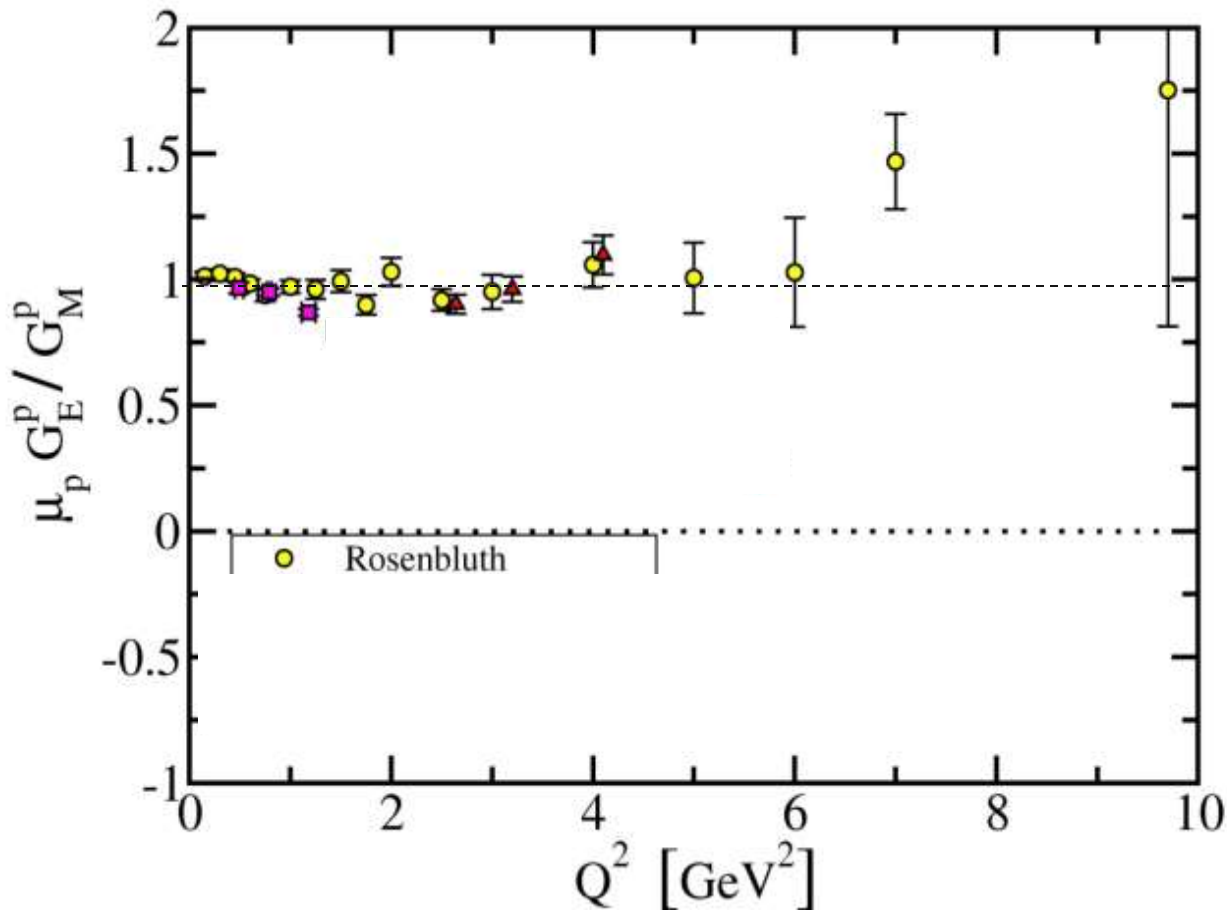


Distribution of charge and magnetisation within the proton

$$\frac{\mu_p G_E^p(Q^2)}{G_M^p(Q^2)}$$

➤ Data before 1999

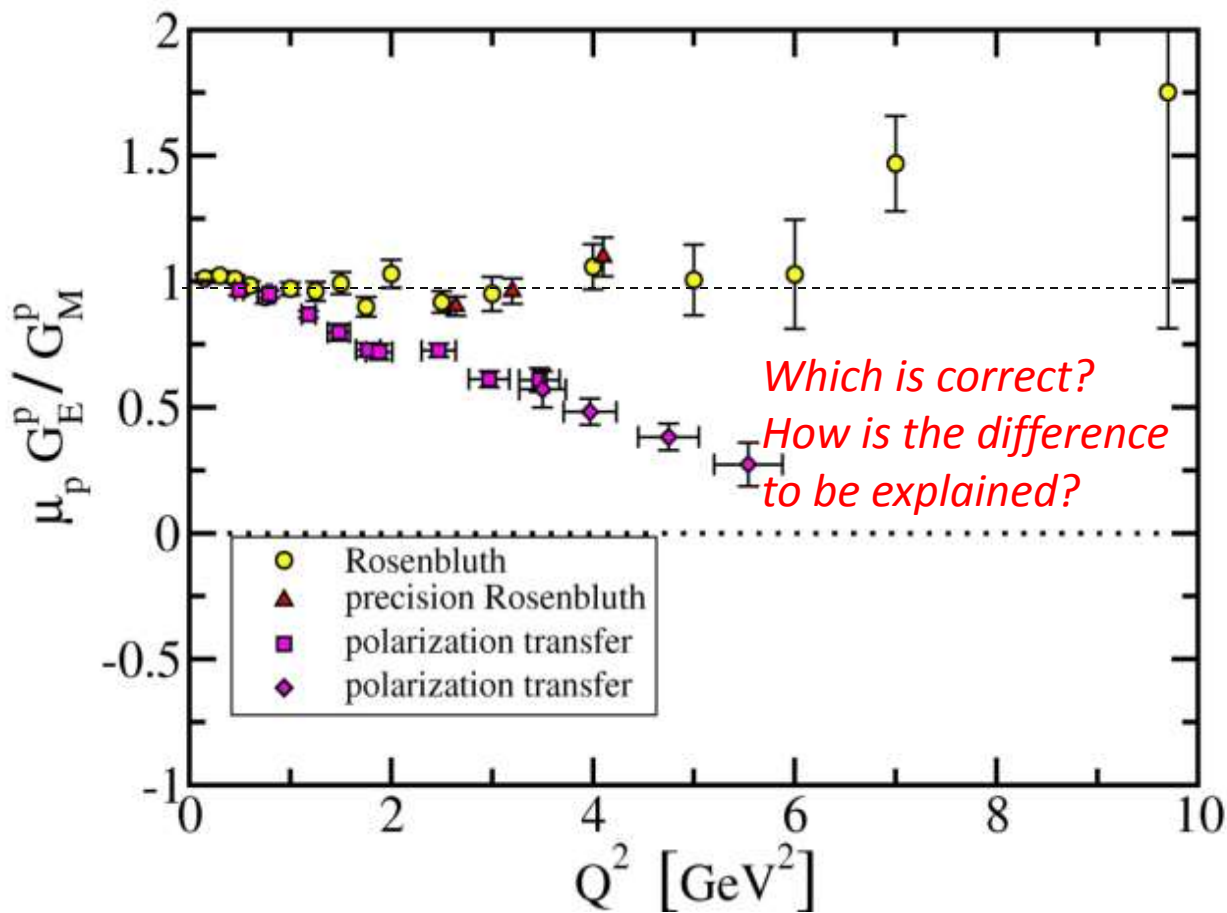
- Looks like the structure of the proton is simple
- Distribution of charge and magnetisation are the same
- Always like that in particle-physics-like pictures of hadrons



Distribution of charge and magnetisation within the proton

$$\frac{\mu_p G_E^p(Q^2)}{G_M^p(Q^2)}$$

- The properties of JLab (high luminosity) enabled a new technique to be employed.
- First data released in 1999 and paint a **VERY DIFFERENT PICTURE**



$$\frac{\mu_p G_E^p(Q^2)}{G_M^p(Q^2)}$$

Distribution of charge is different from distribution of magnetisation

Jlab Highlights

<http://www.jlab.org/highlights/phys.html>

The Electric and Magnetic Elastic Proton Form Factor Ratio G_{Ep}/G_{Mp}

One of the fundamental goals of nuclear physics is to understand the structure and behavior of strongly interacting matter in terms of its basic constituents, quarks and gluons. An important step towards this goal is the characterization of the internal structure of the nucleon; the elastic electric and magnetic form factors of the proton and neutron are key ingredients of this characterization. The elastic electromagnetic form factors are directly related to the charge and current distributions inside the nucleon; these form factors are among the most basic observables of the nucleon.

The challenge of understanding the nucleon's structure and dynamics has occupied a central place in nuclear physics; many experimental and theoretical physicists have spent a considerable amount of effort in the last five decades to understand it. A break-through was made towards this goal in the last decade and a half, when two JLab Hall A experiments extracted the elastic electromagnetic form factor ratio of the proton, GEp/GMp , from the measured recoil proton polarization components, using the polarization transfer method. A third experiment in Hall C at JLab has pushed the highest Q^2 limit to 8.5 GeV 2 using the same method.

The form factor ratio data from all three JLab recoil polarization experiments are shown in Figure 1, which display a strikingly different Q^2 dependence than the Rosenbluth results. The most important feature of the data from JLab is the decrease of the ratio to $Q^2 = 8.5$ GeV 2 , which indicates that GEp falls faster with increasing Q^2 than GMp and demonstrates that the spatial extension of charge is larger than that of magnetization. This is the first definitive experimental indication that the Q^2 dependence of GEp and GMp is different. In the third experiment in Hall C, the ratio is decreasing, however with a strong indication that the linear behavior has softened toward a possible constancy of the ratio at Q^2 values beyond the range covered so far.

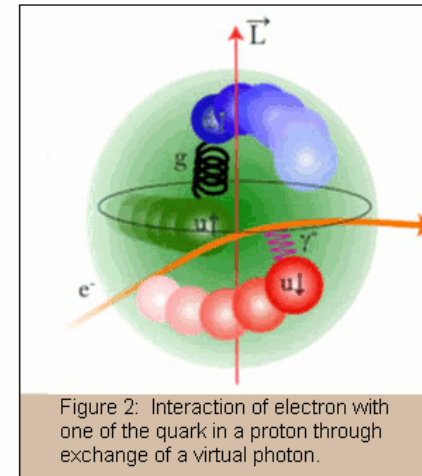


Figure 2: Interaction of electron with one of the quarks in a proton through exchange of a virtual photon.

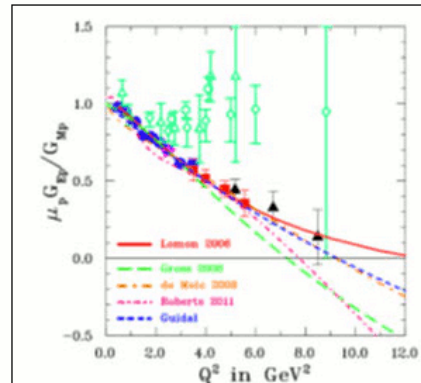


Figure 1: The ratio GEp/GMp obtained by the recoil polarization technique (Punjabi et al. (2005) (filled blue circle), Puckett et al. (2012) (filled red squares) and Puckett et al. (2010) (filled black triangles)) compared to ratio obtained by the Rosenbluth technique (green open points). Theoretical curves from Lomon (2002), Guidal et al. (2005), de Melo et al. (2009), Gross et al. (2008), and Roberts et al. (2009), shown as solid (red), short-dashed (blue), dash-dot (orange), dash (green), and short dash-dot (magenta), respectively.

References:

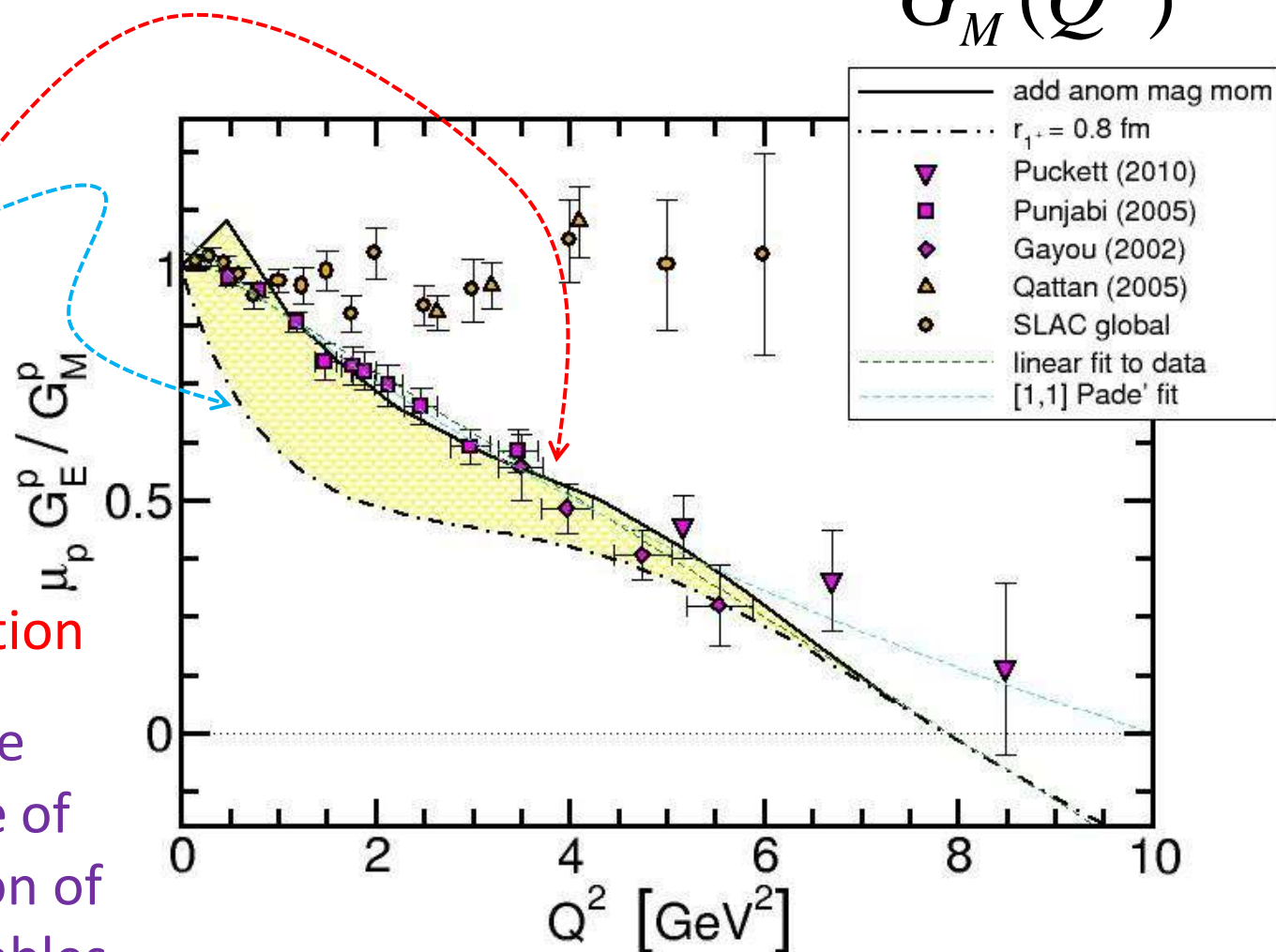
1. M. K. Jones et al., [Phys. Rev. Lett. 84 \(2000\) 1398](#); V. Punjabi et al., [Phys. Rev. C 71 \(2005\) 055202](#)
2. O. Gayou et al., [Phys. Rev. Lett. 88 \(2002\) 092301](#); A.J.R. Puckett et al., [Phys. Rev. C 85 \(2012\) 045203](#)
3. A.J.R. Puckett et al., [Phys. Rev. Lett. 104 \(2010\) 242301](#)
4. C.F. Perdrisat, V. Punjabi and M. Vanderhaeghen, [Prog. Nucl. Part. Phys. 59 \(2007\) 694](#)

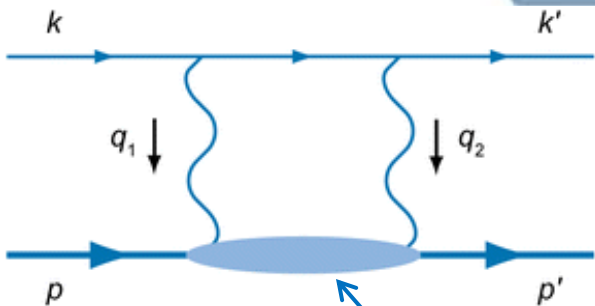
Craig Roberts: Bound state problem in continuum QCD (87p)

Sao Paulo: II Workshop on Perspectives in Nonperturbative QCD, 12-13 May 14

$$\frac{\mu_p G_E^p(Q^2)}{G_M^p(Q^2)}$$

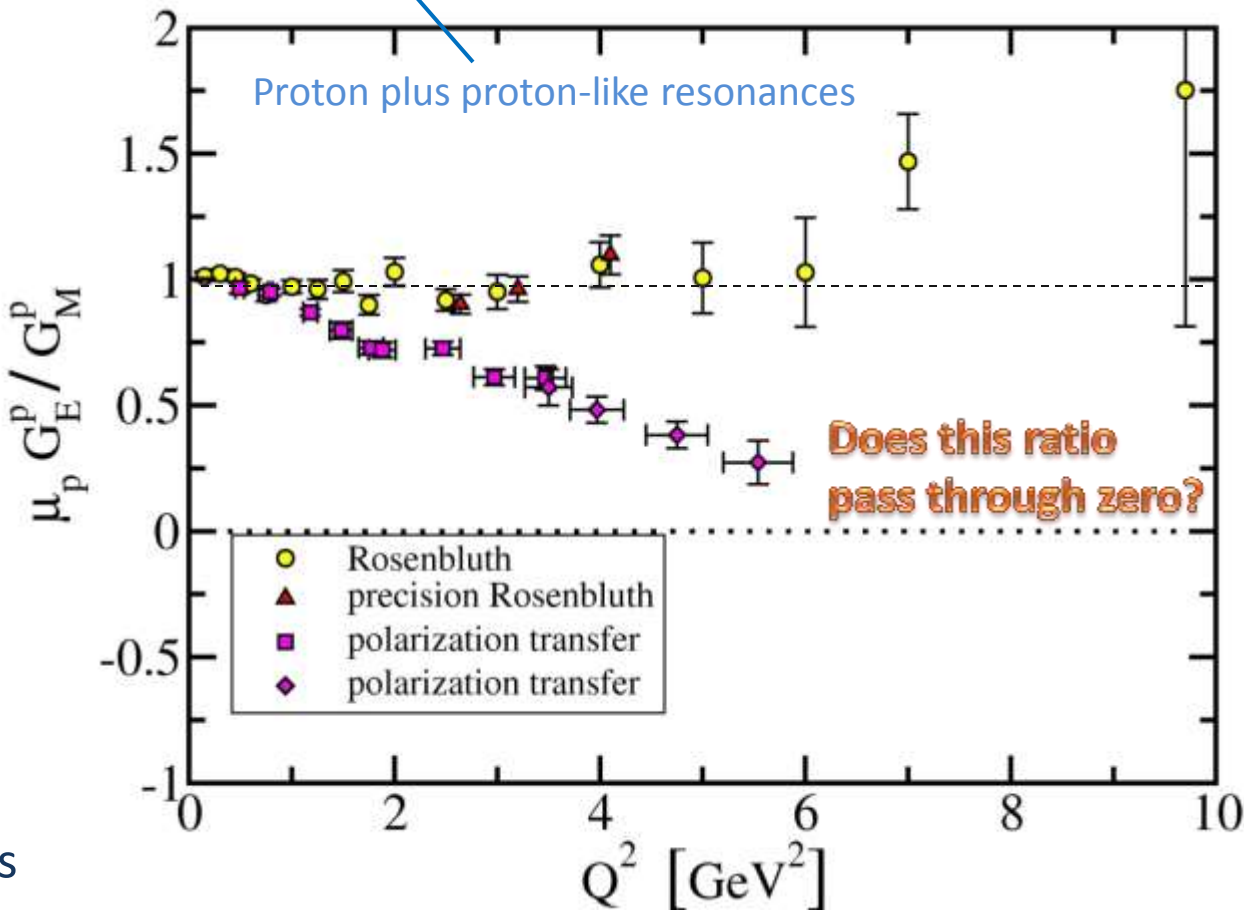
- DSE result Dec 08
- DSE result
 - including the anomalous magnetic moment distribution
- Highlights again the critical importance of DCSB in explanation of real-world observables.





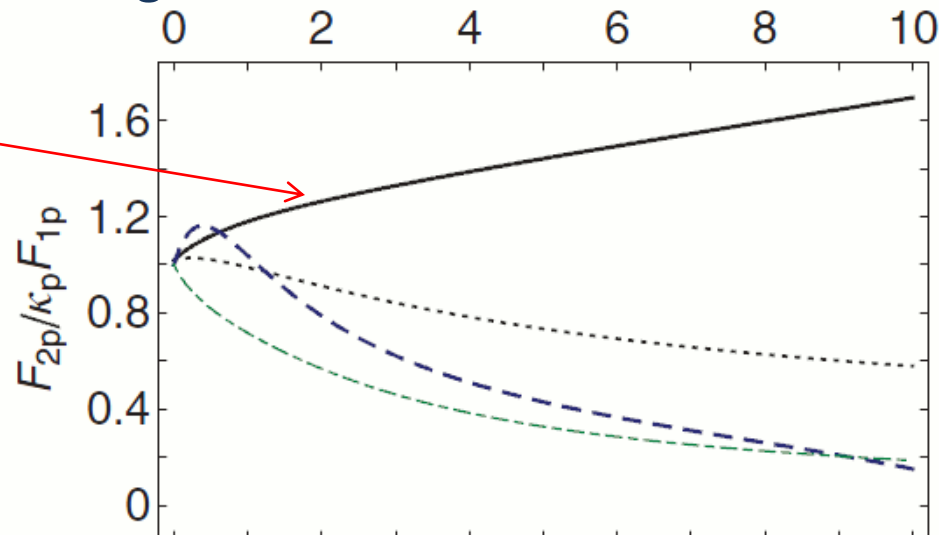
$$\frac{\mu_p G_E^p(Q^2)}{G_M^p(Q^2)}$$

- DSE studies indicate that the *proton has a very rich internal structure*
- The JLab data, obtained using the polarisaton transfer method, are an accurate indication of the behaviour of this ratio
- The pre-1999 data (Rosenbluth) receive large corrections from so-called 2-photon exchange contributions

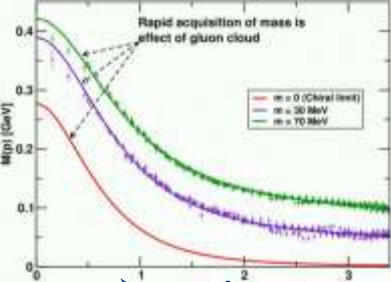


Origin of the zero & its location

- The Pauli form factor is a gauge of the distribution of magnetization within the proton. Ultimately, this magnetisation is carried by the dressed quarks and influenced by correlations amongst them, which are expressed in the Faddeev wave function.
- If the dressed quarks are described by a momentum-independent mass function, $M=\text{constant}$, then they behave as Dirac particles with constant Dirac values for their magnetic moments and produce a hard Pauli form factor.

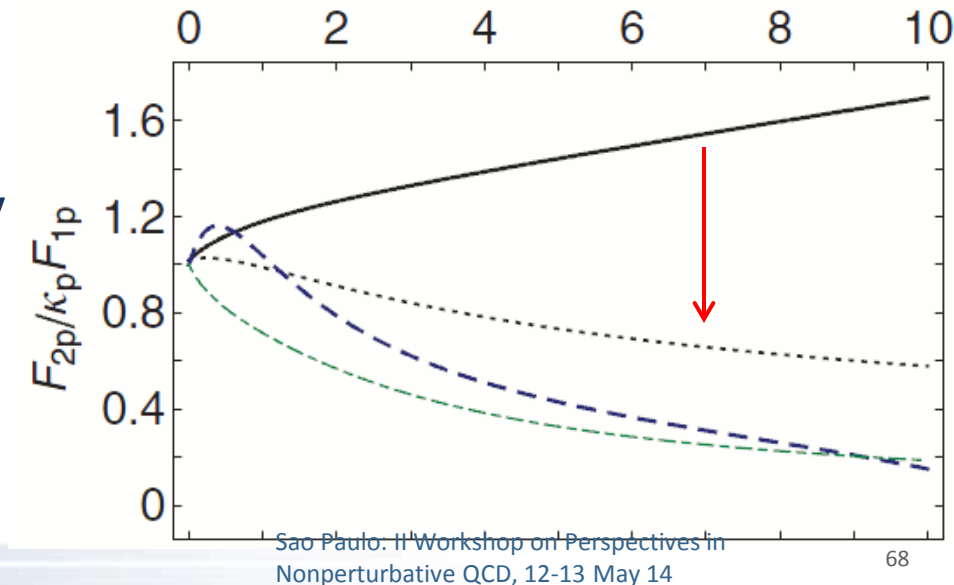


Origin of the zero & its location



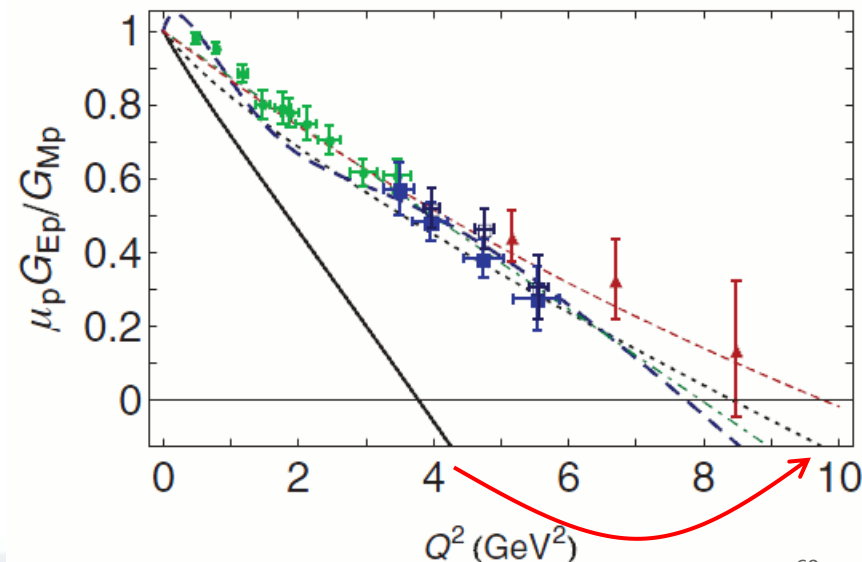
- Alternatively, suppose that the dressed quarks possess a momentum-dependent mass function, $M=M(p^2)$, which is large at infrared momenta but vanishes as their momentum increases.
- At small momenta they will then behave as constituent-like particles with a large magnetic moment, but their mass and magnetic moment will drop toward zero as the probe momentum grows. (Remember: Massless fermions do not possess a measurable magnetic moment)
- Such dressed quarks produce a proton Pauli form factor that is large for $Q^2 \sim 0$ but drops rapidly on the domain of transition between nonperturbative and perturbative QCD, to give a very small result at large Q^2 .

Craig Roberts: Bound state problem in continuum QCD (87p)



Origin of the zero & its location

- The precise form of the Q^2 dependence will depend on the evolving nature of the angular momentum correlations between the dressed quarks.
- From this perspective, existence, and location if so, of the zero in
$$\mu_p G_{Ep}(Q^2)/G_{Mp}(Q^2)$$
are a fairly direct measure of the location and width of the transition region between the nonperturbative and perturbative domains of QCD as expressed in the momentum dependence of the dressed-quark mass function.
- Hard, $M=\text{constant}$
→ Soft, $M=M(p^2)$



Nucleon and Roper electromagnetic elastic and transition form factors, D. J. Wilson, et al., arXiv:1112.2212 [nucl-th], Phys. Rev. C85 (2012) 025205 [21 pages]

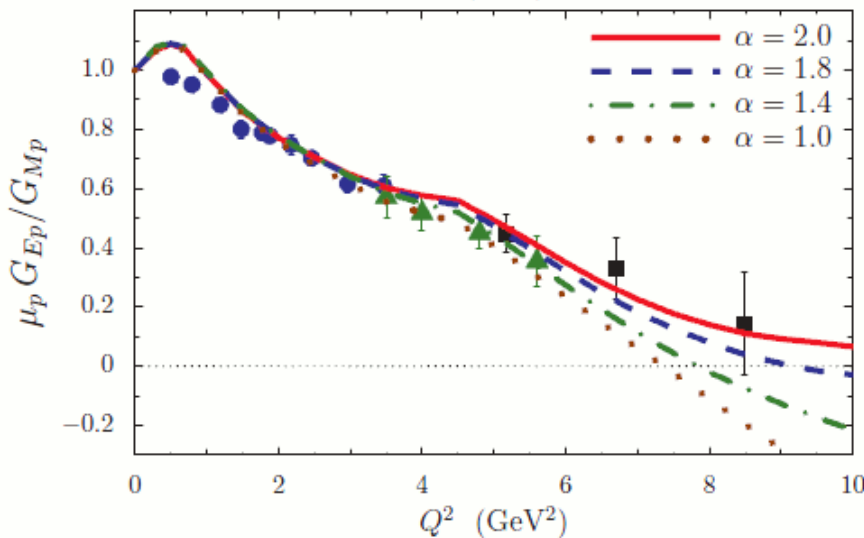
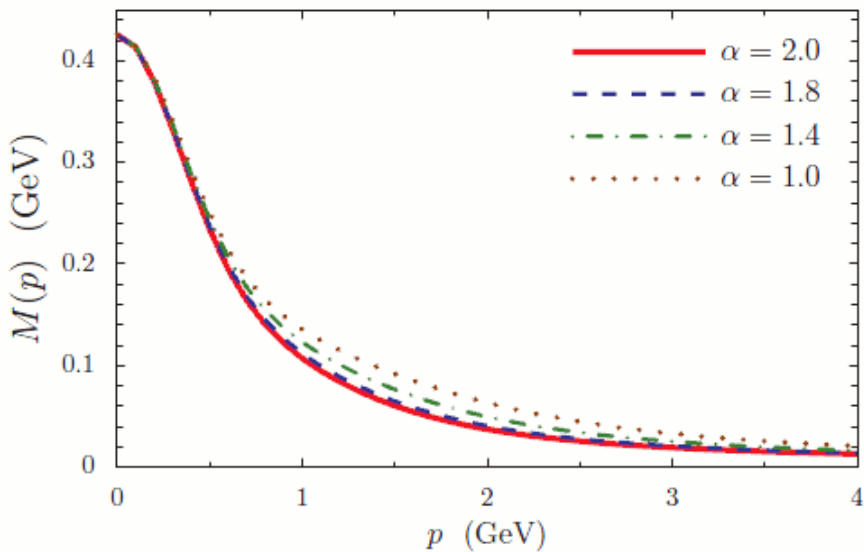
I.C. Cloët, C.D. Roberts, A.W. Thomas,
Phys. Rev. Lett. 111 (2013) 101803 [5 pages]

Origin of the zero & its location

- One can anticipate that a mass function which rapidly becomes partonic—namely, is very soft—will not produce a zero
- We've seen that a constant mass function produces a zero at a small value of Q^2
- And also seen and know that a mass function which resembles that obtained in the best available DSE studies and via lattice-QCD simulations produces a zero at a location that is consistent with extant data.
- There is opportunity here for very constructive feedback between future experiments and theory.

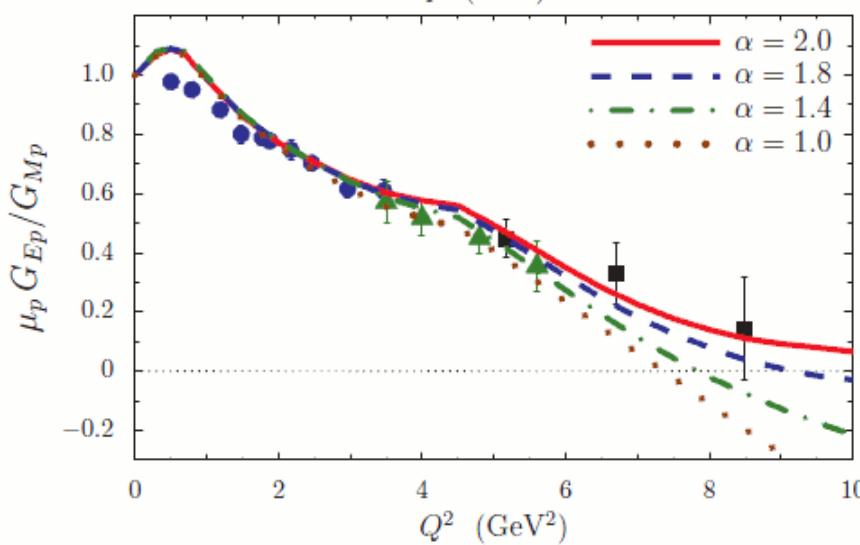
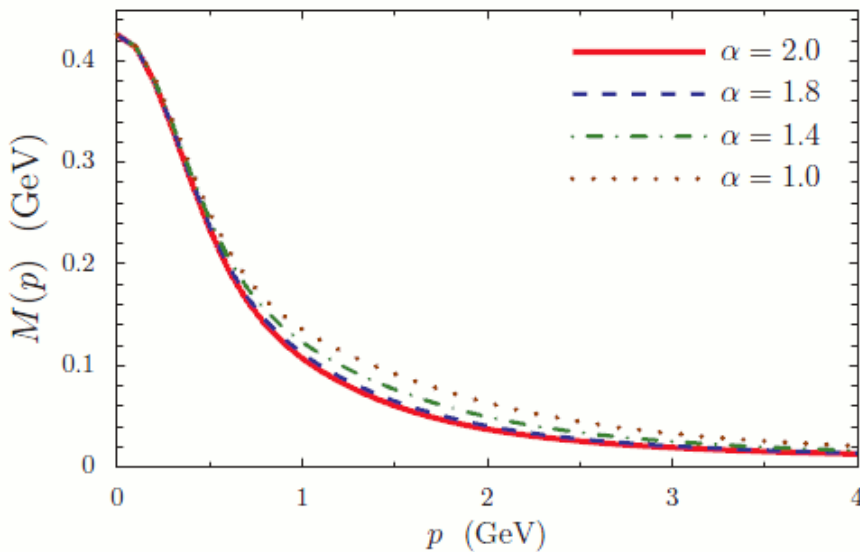
Visible Impacts

$$S(p) = \frac{Z(p^2)}{i\gamma \cdot p + M(p^2)}$$



- Apparently small changes in $M(p)$ within the domain $1 < p(\text{GeV}) < 3$ have striking effect on the proton's electric form factor
- The possible existence and location of the zero is determined by behaviour of $Q^2 F_2^p(Q^2)$
- Like the pion's PDA, $Q^2 F_2^p(Q^2)$ measures the rate at which dressed-quarks become parton-like:
 - ✓ $F_2^p = 0$ for bare quark-partons
 - ✓ Therefore, G_E^p can't be zero on the bare-parton domain

Visible Impacts of DCSB



$$S(p) = \frac{Z(p^2)}{i\gamma \cdot p + M(p^2)}$$

➤ Follows that the

- ✓ possible existence
- ✓ and location

of a zero in the ratio of proton elastic form factors

$[\mu_p G_{Ep}(Q^2)/G_{Mp}(Q^2)]$
 are a direct measure of the nature of
 the quark-quark interaction in the
 Standard Model.

Leads to *Prediction neutron:proton*
 $G_{En}(Q^2) > G_{Ep}(Q^2)$ at $Q^2 > 4\text{GeV}^2$

Flavor Decomposition of the Elastic Nucleon Electromagnetic Form Factors

Abstract

References

Citing Articles (11)

Download: PDF (200 kB) Buy this article Export: BibTeX or EndNote (RIS)

G. D. Cates¹, C. W. de Jager², S. Riordan³, and B. Wojtsekhowski^{2,*}

¹*University of Virginia, Charlottesville, Virginia 22903, USA*

²*Thomas Jefferson National Accelerator Facility, Newport News, Virginia 23606, USA*

³*University of Massachusetts, Amherst, Massachusetts 01003, USA*

Received 8 March 2011; published 22 June 2011



Article Available via CHORUS Pilot

[Download Accepted Manuscript](#)

The u - and d -quark contributions to the elastic nucleon electromagnetic form factors have been determined by using experimental data on G_E^n , G_M^n , G_E^D , and G_M^D . Such a flavor separation of the form factors became possible up to negative four-momentum transfer squared $Q^2=3.4 \text{ GeV}^2$ with recent data on G_E^n from Hall A at Jefferson Lab. For Q^2 above 1 GeV^2 , for both the u and the d quark, the ratio of the Pauli and Dirac form factors, F_2/F_1 , was found to be almost constant in sharp contrast to the behavior of F_2/F_1 for the proton as a whole. Also, again for $Q^2>1 \text{ GeV}^2$, both F_2^d and F_1^d are roughly proportional to $1/Q^4$, whereas the dropoff of F_2^u and F_1^u is more gradual.

© 2011 American Physical Society

URL: <http://link.aps.org/doi/10.1103/PhysRevLett.106.252003>

DOI: [10.1103/PhysRevLett.106.252003](https://doi.org/10.1103/PhysRevLett.106.252003)

PACS: 14.20.Dh, 13.40.Gp, 24.70.+s, 25.30.Bf

Discovering Diquarks

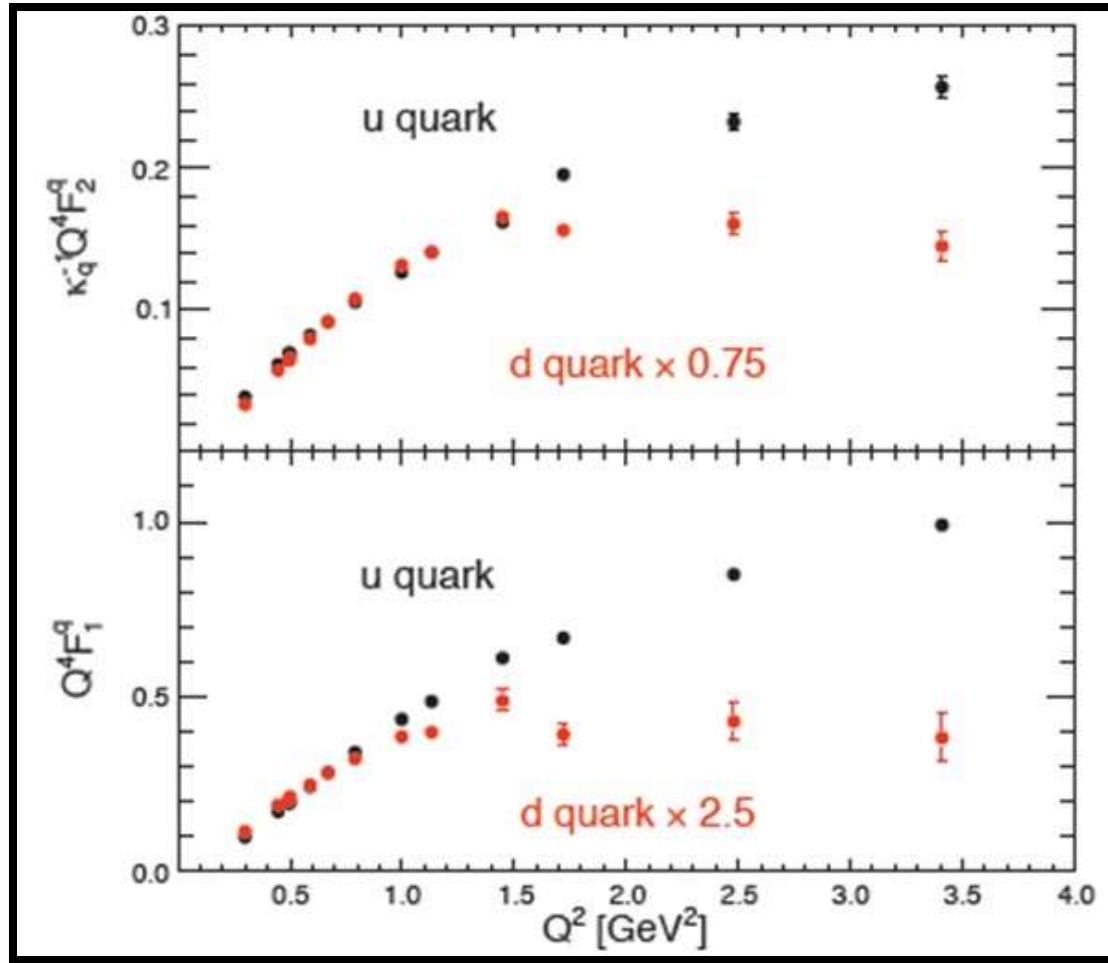


Flavor separation of proton form factors

$$Q^4 F_2^q / \kappa$$

Cates, de Jager,
Riordan, Wojtsekhowski,
PRL 106 (2011) 252003

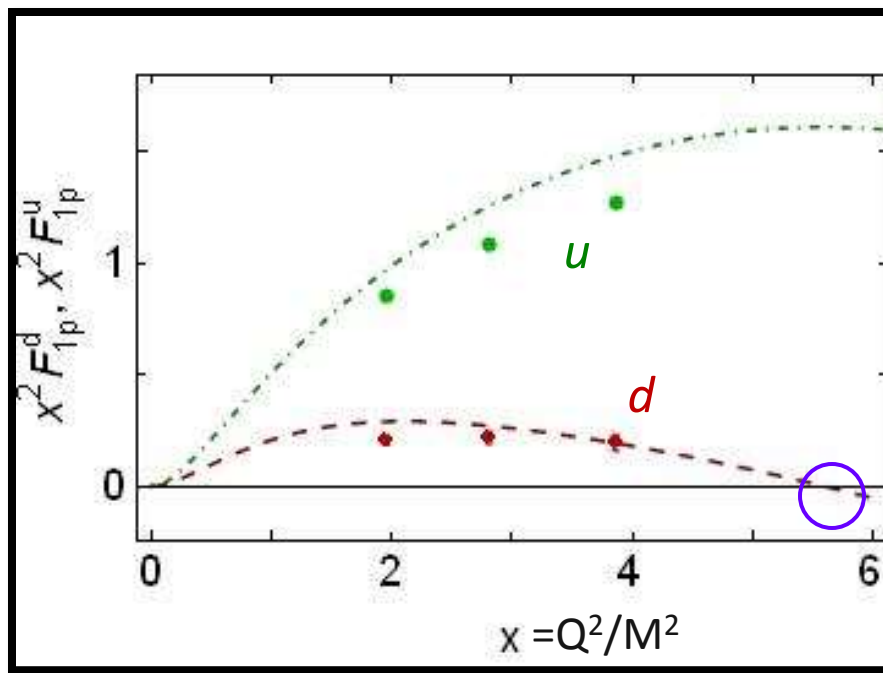
$$Q^4 F_1^q$$



➤ Very different behavior for u & d quarks

Means apparent scaling in proton F_2/F_1 is *purely accidental*

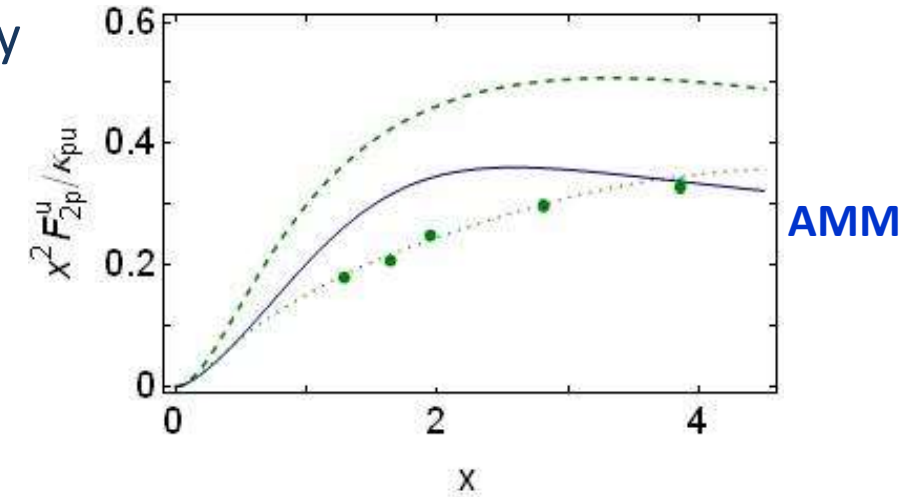
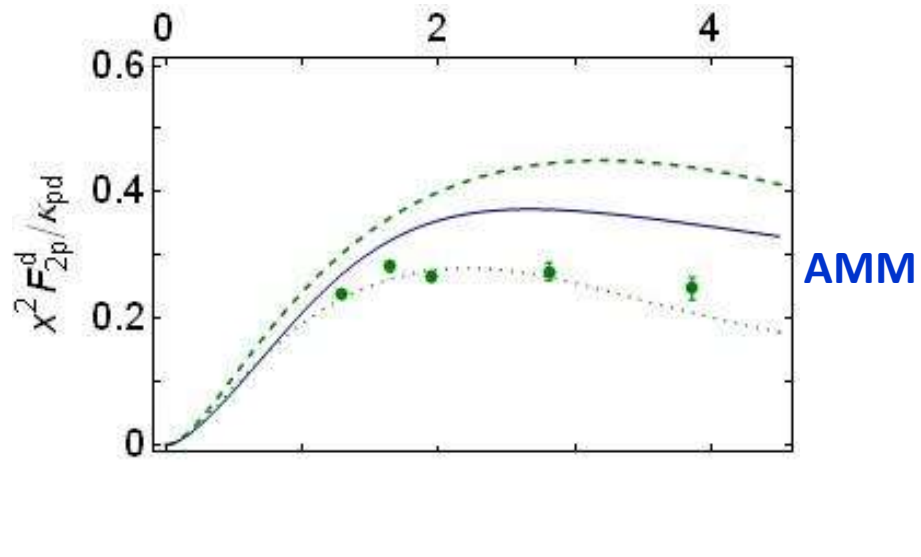
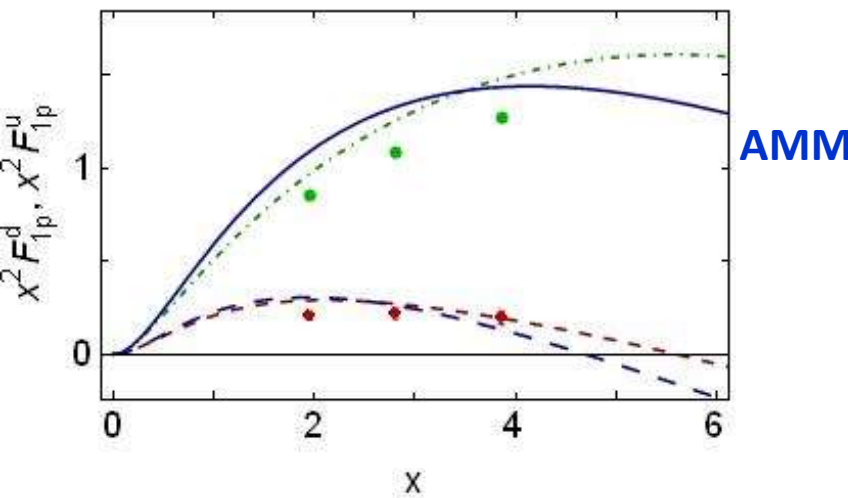
Diquark correlations!



- Poincaré covariant Faddeev equation
 - Predicts scalar and axial-vector diquarks
- Proton's singly-represented d -quark more likely to be struck in association with 1^+ diquark than with 0^+
 - form factor contributions involving 1^+ diquark are softer

- Doubly-represented u -quark is predominantly linked with harder 0^+ diquark contributions
- Interference produces zero in Dirac form factor of d -quark in proton
 - Location of the zero depends on the relative probability of finding 1^+ & 0^+ diquarks in proton
 - Correlated, e.g., with valence d/u ratio at $x=1$

Diquark correlations!



- Adding dressed-quark AMM (sensibly modifying the current operator) can quantitatively improve the description of data
- But it's the presence of diquark correlations that explains the difference between u- and d-quark distributions within the nucleon



Far valence domain

$x \approx 1$

Far valence domain

$x \simeq 1$

- Endpoint of the far valence domain: $x \simeq 1$, is especially significant
 - All familiar PDFs vanish at $x=1$; but ratios of any two need not
 - Under DGLAP evolution, the value of such a ratio is invariant.
- Thus, e.g.,
 - $\lim_{x \rightarrow 1} d_v(x)/u_v(x)$
is unambiguous, scale invariant, nonperturbative feature of QCD.
 \therefore keen discriminator between frameworks
that claim to explain nucleon structure.
- Furthermore, Bjorken- $x=1$ corresponds strictly to the situation in which the invariant mass of the hadronic final state is precisely that of the target; viz., elastic scattering.
 - \therefore Structure functions inferred experimentally on $x \simeq 1$
are determined theoretically by target's elastic form factors.

Neutron Structure Function at high-x

➤ Valence-quark distributions at $x=1$

- Fixed point under DGLAP evolution
- Strong discriminator between theories

➤ Algebraic formula

$$\frac{d_v(x)}{u_v(x)} \Big|_{x \rightarrow 1} = \frac{P_1^{p,d}}{P_1^{p,u}} = \frac{\frac{2}{3} P_1^{p,a} + \frac{1}{3} P_1^{p,m}}{P_1^{p,s} + \frac{1}{3} P_1^{p,a} + \frac{2}{3} P_1^{p,m}}$$

- $P_1^{p,s}$ = contribution to the proton's charge arising from diagrams with a scalar diquark component in both the initial and final state
- $P_1^{p,a}$ = kindred axial-vector diquark contribution
- $P_1^{p,m}$ = contribution to the proton's charge arising from diagrams with a different diquark component in the initial and final state.

$$\frac{d_v(x)}{u_v(x)} \Big|_{x \rightarrow 1}, \quad \text{where}$$

$$\frac{d_v(x)}{u_v(x)} = \frac{4 \frac{F_2^n(x)}{F_2^p(x)} - 1}{4 - \frac{F_2^n(x)}{F_2^p(x)}}$$

Measures relative strength
of axial-vector/scalar
diquarks in proton

Neutron Structure Function at high-x

*Deep inelastic scattering
– the Nobel-prize winning
quark-discovery experiments*

Reviews:

➤ S. Brodsky et al.

NP B441 (1995)

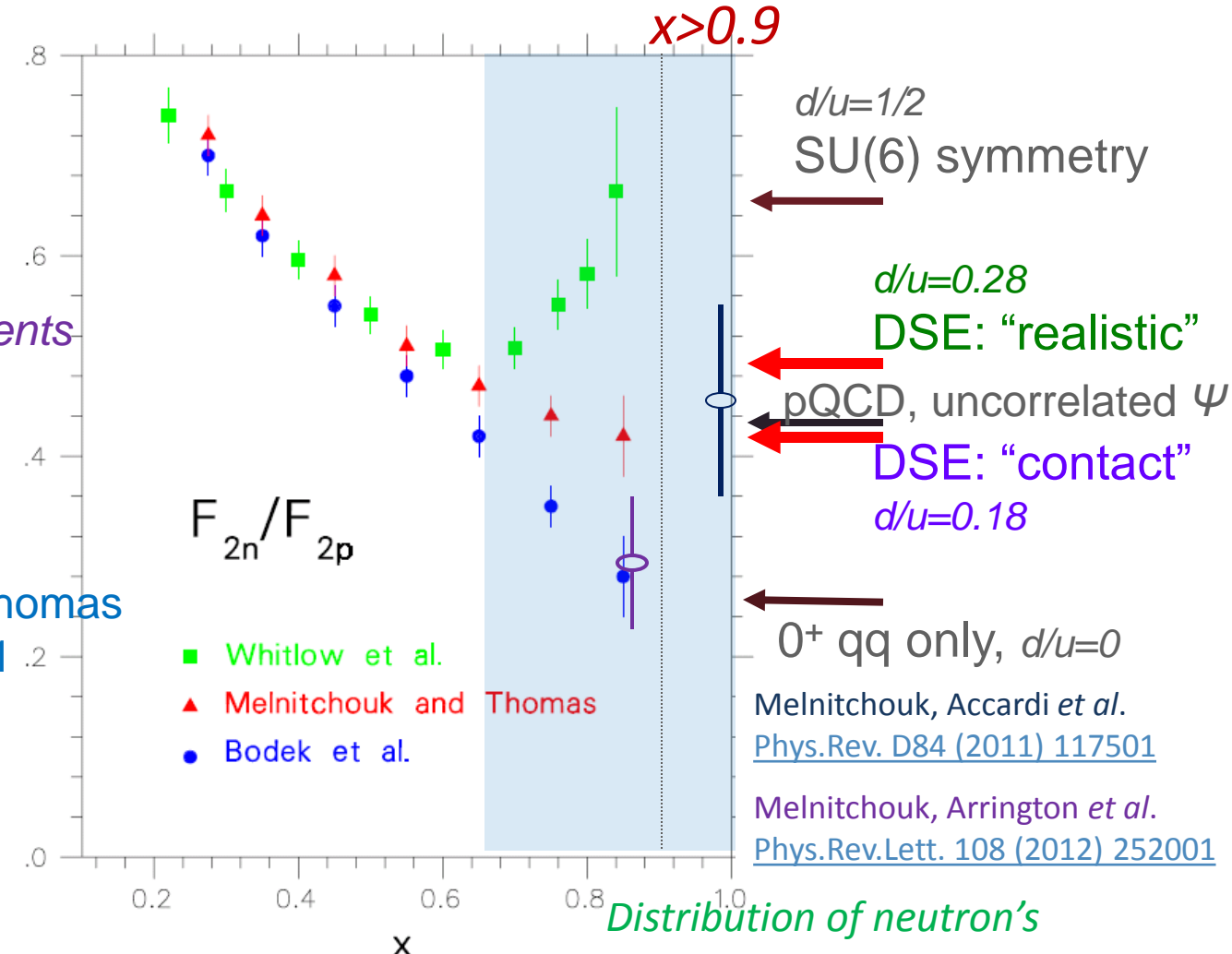
➤ W. Melnitchouk & A.W.Thomas

PL B377 (1996) 11

➤ N. Isgur, PRD 59 (1999)

➤ R.J. Holt & C.D. Roberts

RMP (2010)



*Distribution of neutron's
momentum amongst quarks
on the valence-quark domain*

Neutron Structure Function at high-x

NB.

Deep inelastic scattering
– the Nobel prize winning
quark-discovery experiments

Reviews:

➤ S. Brodsky et al.

NP B441 (1995)

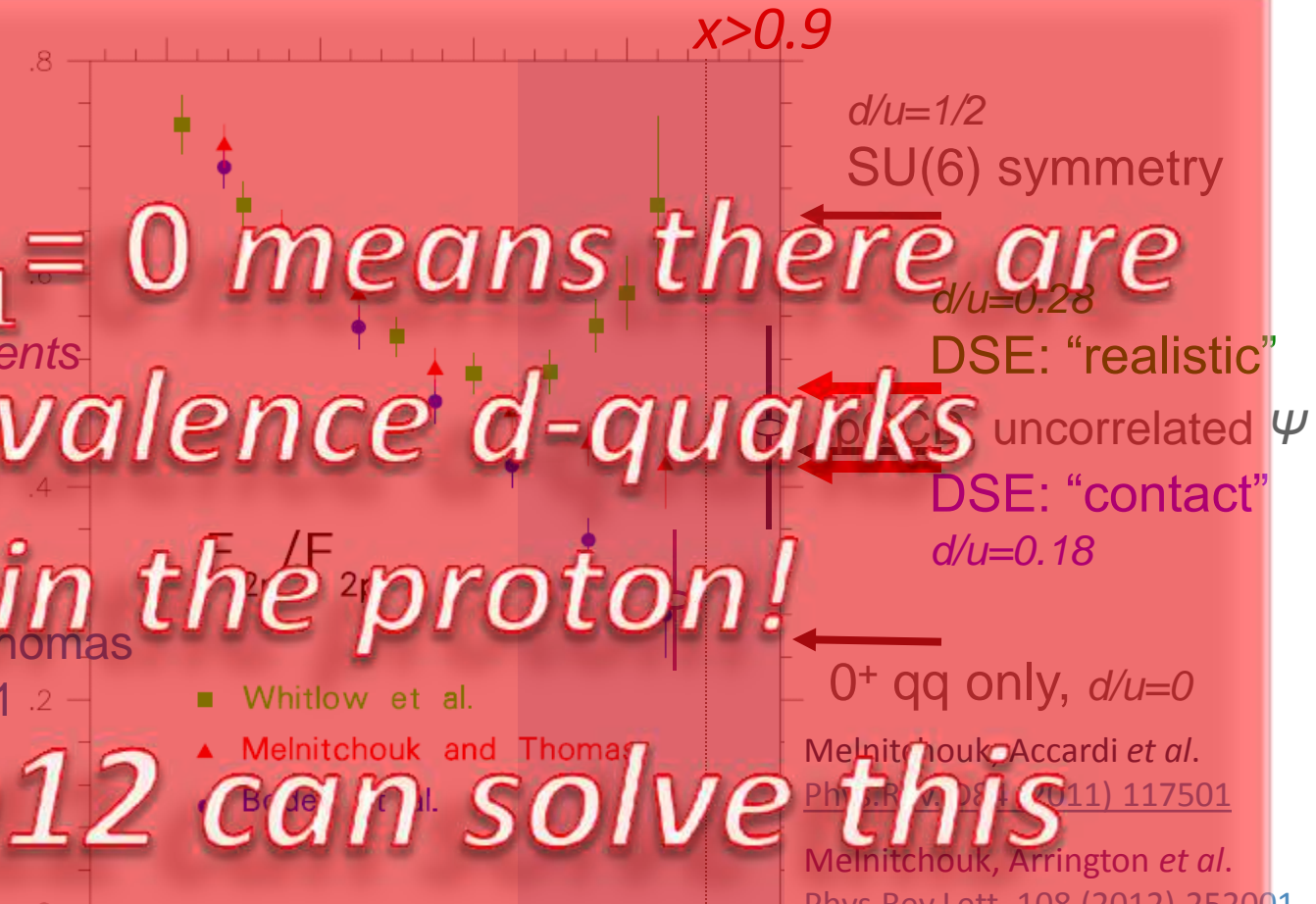
➤ W. Melnitchouk & A.W.Thomas

PL B377 (1996) 11

➤ N. Isgur, PRD 59 (1999)

➤ R.J. Holt & C.D. Roberts

RMP (2010)



JLab12 can solve this enigma

Distribution of neutron's momentum amongst quarks

on the valence-quark domain



Nucleon spin structure at very high x

Craig D. Roberts ^{a,*}, Roy J. Holt ^a, Sebastian M. Schmidt ^b

^a Physics Division, Argonne National Laboratory, Argonne, IL, 60439, USA

^b Institute for Advanced Simulation, Forschungszentrum Jülich and JARA, D-52425 Jülich, Germany

ARTICLE INFO

Article history:

Received 6 August 2013

Received in revised form 10 September 2013

Accepted 18 September 2013

Available online 25 September 2013

Editor: A. Ringwald

Keywords:

Continuum strong QCD

Diquark correlations

Dynamical chiral symmetry breaking

Dyson–Schwinger equations

Nucleon longitudinal spin asymmetries

Parton distribution functions

Valence quarks at very high x

ABSTRACT

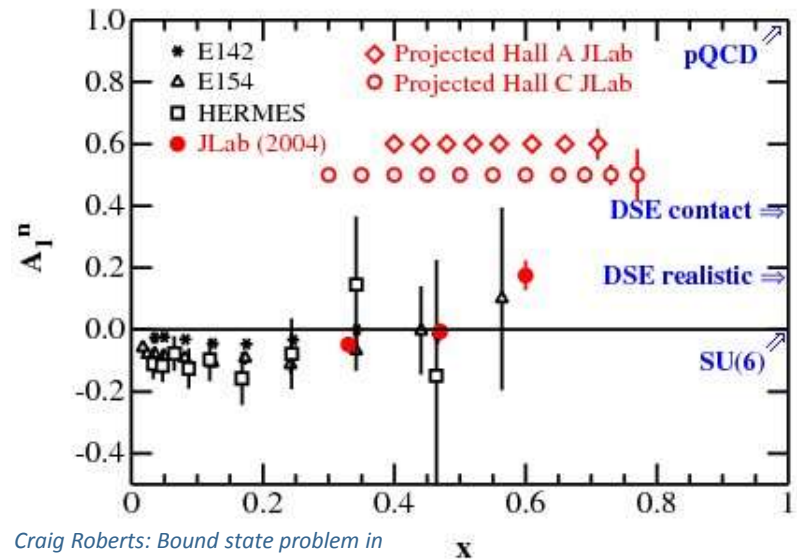
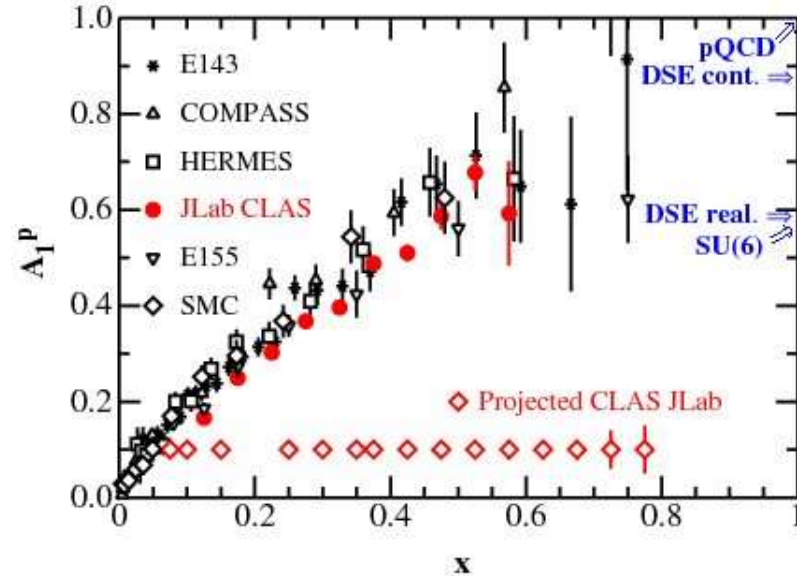
Dyson–Schwinger equation treatments of the strong interaction show that the presence and importance of nonpointlike diquark correlations within the nucleon are a natural consequence of dynamical chiral symmetry breaking. Using this foundation, we deduce a collection of simple formulae, expressed in terms of diquark appearance and mixing probabilities, from which one may compute ratios of longitudinal-spin-dependent *u*- and *d*-quark parton distribution functions on the domain $x \simeq 1$. A comparison with predictions from other approaches plus a consideration of extant and planned experiments shows that the measurement of nucleon longitudinal spin asymmetries on $x \simeq 1$ can add considerably to our capacity for discriminating between contemporary pictures of nucleon structure.

© 2013 Elsevier B.V. All rights reserved.

Spin structure on $x \simeq 1$

Craig Roberts: Bound state problem in continuum QCD (87p)

Sao Paulo: II Workshop on Perspectives in Nonperturbative QCD, 12–13 May 14

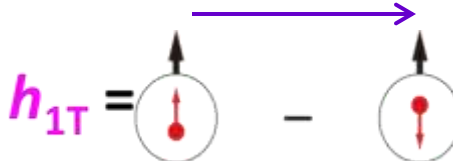


Nucleon spin structure at very high x

- Similar formulae for nucleon longitudinal structure functions.
- Plainly, existing data cannot distinguish between modern pictures of nucleon structure
- Empirical results for nucleon longitudinal spin asymmetries on $x \approx 1$ promise to add greatly to our capacity for discriminating between contemporary pictures of nucleon structure.

NB. pQCD is actually model-dependent: assumes $SU(6)$ spin-flavour wave function for the proton's valence-quarks and the corollary that a hard photon may interact only with a quark that possesses the same helicity as the target.

Direction of motion



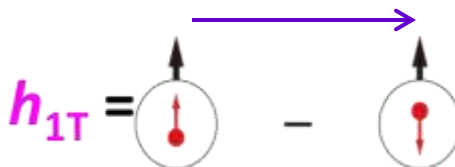
→ Nucleon Spin
→ Quark Spin

Tensor Charge: $\sigma_{\mu\nu}$ current

$$\delta q = \int_0^1 dx (h_1^q(x) - h_1^{\bar{q}}(x))$$

- h_{1T} = distribution of transversely polarized quarks inside a transversely polarised proton
- δq = Light-front number-density of quarks with transverse polarisation parallel to that of the proton *minus* that of quarks with transverse polarisation antiparallel
 - Bias in quark polarisation induced by polarisation of parent proton
- Value of tensor charge places constraints on some extensions of the Standard Model <[PRD85 \(2012\) 054512](#)>
- Current knowledge of transversity: SIDIS @HERMES, COMPASS, JLab
- No gluon transversity distribution => transversity is suppressed at low-x, hence large-x behavior important => JLab12 a useful tool. Transversity will be measured at JLab12 (Hall-A E12-09-018-SIDIS; CLAS12; and SoLID)

Direction of motion

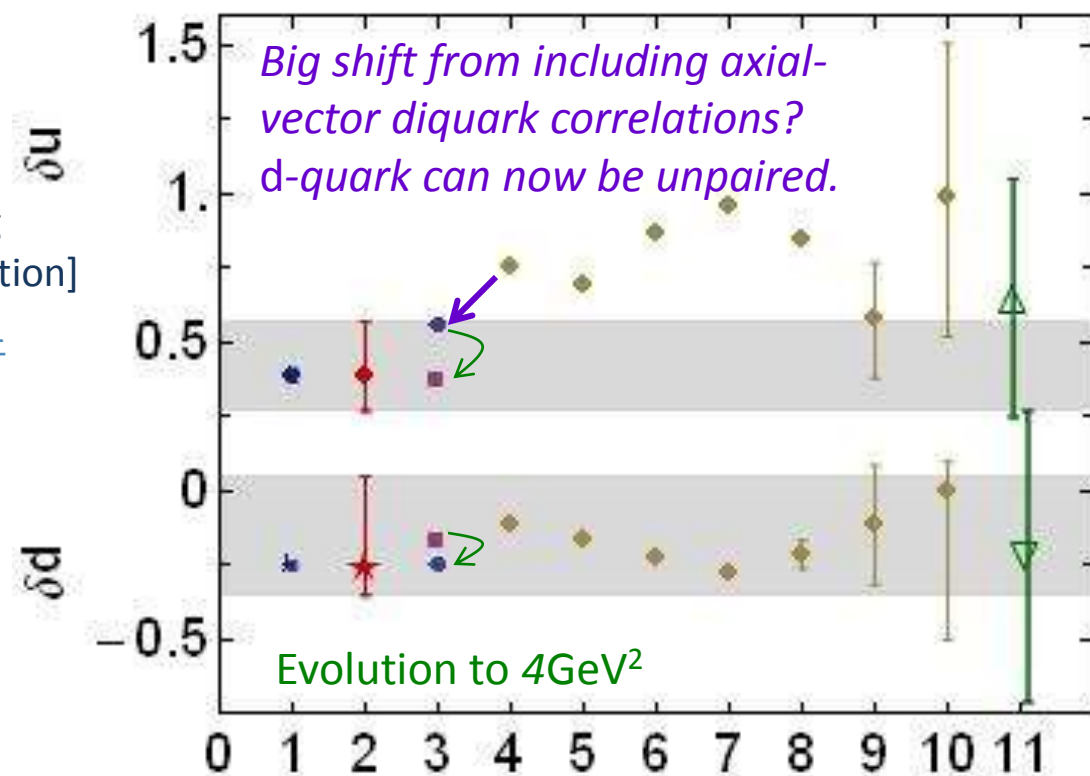


- Nucleon Spin
- Quark Spin

Tensor Charge: $\sigma_{\mu\nu}$ current

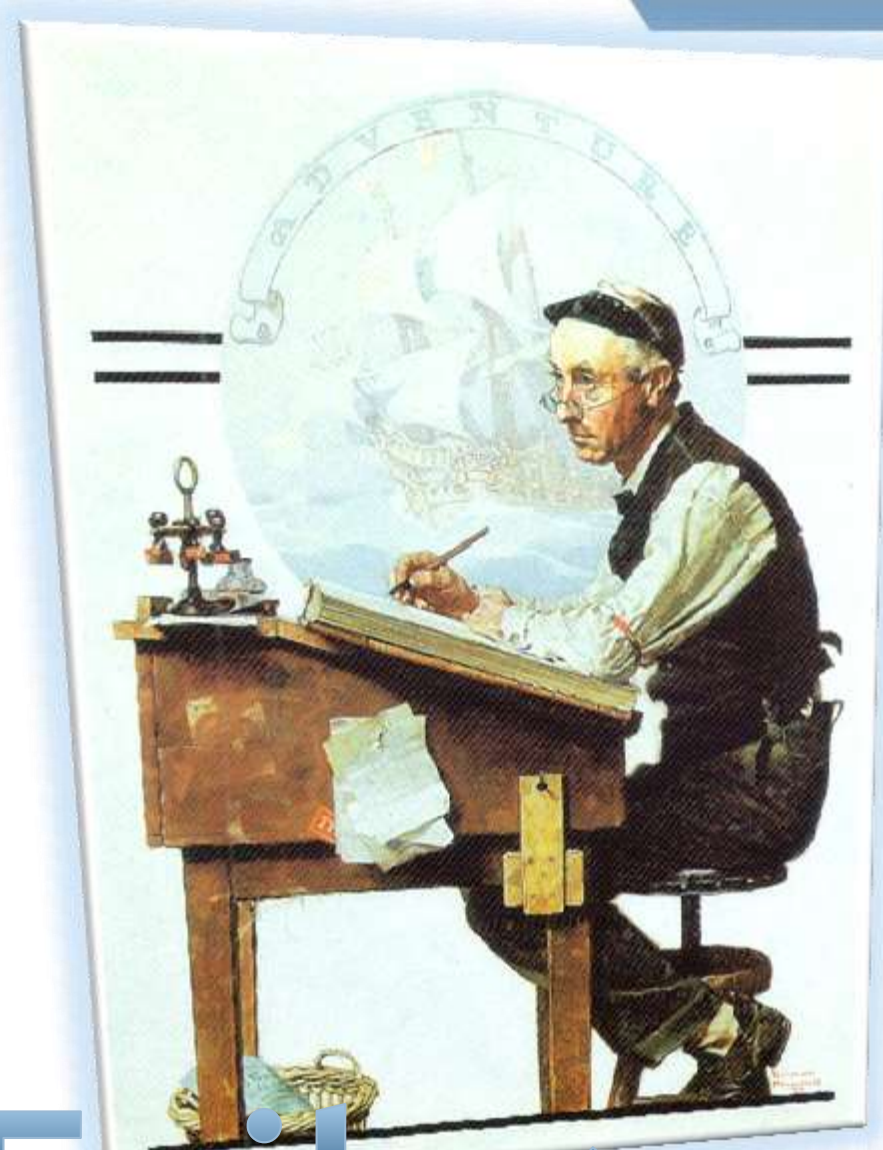
$$\delta q = \int_0^1 dx (h_1^q(x) - h_1^{\bar{q}}(x))$$

1. Jlab 12 Projection
2. Anselmino *et al.*, [1303.3822 \[hep-ph\]](#)
3. Pitschmann *et al.* (DSE) (2014) [including axial-vector diquarks *but* contact interaction]
4. Hecht *et al.* (DSE), [PRC64 \(2001\) 025204](#) [only scalar diquarks]
5. Cloët *et al.*, [PLB659 \(2008\) 214](#)
6. Pasquini *et al.*, [PRD76 \(2007\) 034020](#)
7. Wakamatsu, [PLB653 \(2007\) 398](#)
8. Gockeler *et al.*, [PLB627 \(2005\) 113](#)
9. Gamberg *et al.*, [PRL 87 \(2001\) 242001](#)
10. He *et al.*, [PRD52 \(1995\) 2960](#)
11. Bacchetta *et al.*, [JHEP 1303 \(2013\) 119](#)



Epilogue

Craig Roberts: Bound state problem in continuum QCD (87p)



Sao Paulo: II Workshop on Perspectives in
Nonperturbative QCD, 12-13 May 14

DSEs: A practical, predictive, unifying tool for fundamental physics

- Exact results proved in QCD, amongst them:
 - ✓ Quarks are not Dirac particles and gluons are nonperturbatively massive
 - ✓ Dynamical chiral symmetry breaking is a fact.
It's responsible for 98% of the mass of visible matter in the Universe
 - ✓ Goldstone's theorem is fundamentally an expression of equivalence between the one-body problem and the two-body problem in the pseudoscalar channel
 - ✓ Confinement is a dynamical phenomenon
It cannot in principle be expressed via a potential
 - ✓ The list goes on ...

McLerran & Pisarski
[arXiv:0706.2191 \[hep-ph\]](https://arxiv.org/abs/0706.2191)

- DSEs are a single framework, with IR model-input turned to advantage,
“almost unique in providing an unambiguous path from a defined interaction → Confinement & DCSB → Masses → radii → form factors → distribution functions → etc.”